



Study of the correlation between adhesive curing state and handling of digital instrument display for automotive industry

João Pedro dos Santos Gomes

Thesis to obtain the Master's Degree in
Materials Engineering

Supervisor(s):

Prof. Ana Clara Lopes Marques

Eng. André Felipe de Jesus Lopes Ruza

Examination Committee

Chairperson: Prof. José Paulo Sequeira Farinha

Supervisor: Prof. Ana Clara Lopes Marques

Vogal: Dr. Diana Cristina Morais da Silva Pereira

Vogal: Prof. Pedro Miguel de Almeida Areias

November 2022

Acknowledgments

I would like thanks my supervisors, Ana Marques and André Ruza for the close mentoring given for the last few months; everyone at Visteon's Bonding Technology Centre; everyone involved at IST, and finally my whole family and friends for their support.

Abstract

This research was developed within the company Visteon, having as main objectives the study of the curing state and of the mechanical behavior of three structural adhesives and the selection of the best performing adhesive during the assembly process of an automotive display.

The success of joint adhesion depends not only on the adhesives, but also on the substrate used as well as its surface preparation. Consequently, the study was initiated by measuring the surface free energy on three substrates, to assess the substrate wettability when using isopropanol cleaning and plasma pre-treatment. For the adhesive's characterization, Shore A hardness, compression tests and lap shear tests were performed. The shear tests allowed to identify the joints failure mode and to verify the influence of the two surface pre-treatments on the strength of each adhesive.

Forces resulting from pallet movement and from screwing processes were identified as the main forces applied to the display during production. Two tests were developed to reproduce and quantify the two main forces resulting from the assembly process.

Using a real display as an example, it was estimated a curing time before advancing to the next process step. Analyzing all the results obtained throughout the study, it was possible to select the best performing in assembly process.

Keywords: structural adhesive, adhesive joint, surface pre-treatment, automotive display, mechanical properties.

Resumo

Esta investigação foi desenvolvida dentro da empresa Visteon, tendo como principais objetivos estudo do estado de cura e do comportamento mecânico de quatro adesivos estruturais e a seleção do adesivo com melhor desempenho durante o processo de montagem de um *display* automóvel.

O sucesso da adesão das juntas depende não só dos adesivos, mas também do substrato utilizado, bem como da sua preparação da superfície. Consequentemente, o estudo foi iniciado através da medição da energia livre de superfície em três substratos, para avaliar a molhabilidade do substrato ao utilizar a limpeza de isopropanol e o pré-tratamento de plasma. Para a caracterização do adesivo, foram realizados testes de dureza Shore A, ensaios de compressão e ensaios de corte. Ensaios de corte permitiram identificar o modo de falha das juntas adesivas e verificar a influência dos dois pré-tratamentos de superfície nas tensões obtidas para cada adesivo.

As forças resultantes do movimento das paletes e dos processos de aparafusamento foram identificadas como as principais forças aplicadas aos *displays* durante a produção. Foram desenvolvidos dois testes simples, mas realistas para reproduzir e quantificar as duas forças principais resultantes do processo de montagem.

Utilizando um *display* automóvel real como exemplo, foi estimado o tempo de cura antes de avançar para o próximo processo. Analisando todos os resultados obtidos ao longo do estudo, foi possível selecionar o melhor desempenho no processo de montagem.

Palavras-Chave: adesivo estrutural, junta adesiva, pré-tratamento de superfície, *display* automóvel, propriedades mecânicas.

Contents

1. Introduction.....	1
1.1 Context	1
1.2 Visteon.....	2
1.3 Display Assembly Process	2
1.3.1 Structural Bonding	4
1.3.2 Assembly Process Forces	4
1.4 Motivation and Objectives	4
2. State of the Art.....	6
2.1 Adhesives	6
2.1.1 Molecular structure	6
2.1.2 Physical Form.....	7
2.1.3 Mechanical performance	7
2.1.4 Curing Method	7
2.1.5 Chemical Composition.....	8
2.2 Adhesion Theory	11
2.2.1 Adhesive Bonded Joints.....	11
2.2.2 Loading Modes	11
2.2.3 Adhesion forces.....	12
2.2.4 Mechanisms of Adhesion	12
2.2.5 Failure Modes.....	14
2.3 Wettability	14
2.3.1 Contact Angle	14
2.3.2 Surface Free Energy	15
2.4 Surface Preparation.....	16
2.4.1 Surface Preparation Selection.....	16
2.4.2 Pre-treatment Process.....	16
3. Materials and Methodology	18
3.1 Substrate Characterization	18

3.1.1	Surface Free Energy	18
3.2	Adhesive Characterization	21
3.2.1	Hardness Test	21
3.2.2	Compression Test	22
3.2.3	Lap Shear Test	24
3.3	Assembly Forces	28
3.3.1	Screwing Forces	28
3.3.2	Acceleration Forces	29
4.	Results and Discussion	31
4.1	Substrate Characterization	31
4.1.1	Surface Free Energy	31
4.2	Adhesive Characterization	35
4.2.1	Hardness Test	35
4.2.2	Compression Test	36
4.2.3	Lap Shear Test	40
4.3	Assembly Forces	49
4.3.1	Screwing Forces	49
4.3.2	Acceleration Forces	52
6.	Conclusion	57
6.1	Future Studies	58
7.	References	59

List of Figures

Figure 1 - Structural adhesives market value in 2020 and in 2030 (adapted from [2])	1
Figure 2 - Visteon display product [5].....	2
Figure 3 - Display assembly exploded view	3
Figure 4 – Buffer (parts) vs. curing time (h)	3
Figure 5 - Thermoplastic, elastomer, and thermoset molecular structures [8]	6
Figure 6 - Common adhesive joints [17]	11
Figure 7 - Basic loading experienced by adhesive, A) tensile, B) compression, C) tensile-shear, D) cleavage, E) peel (adapted from [19])	12
Figure 8 – A - Mechanical interlocking theory [23]; B - Physical adsorption theory (adapted from [29]); C - Chemical bonding theory (adapted from [24])	13
Figure 9 - Adhesive failure modes [26]	14
Figure 10 - Surface-wetting characterization using contact angle measurements [29]	15
Figure 11 - Contact angle (θ) [36]	18
Figure 12 - Substrates employed in this study: magnesium alloy, painted glass and polycarbonate .	19
Figure 13 - Mobile surface analyzer (Krüss) equipment.....	20
Figure 14 - Piezobrush PZ3 (TDK).....	20
Figure 15 - Standard module and nearfield module	20
Figure 16 - Shore A and Shore D comparison (adapted from [38]).....	21
Figure 17 - 2D hardness sample mold	21
Figure 18 - Hardness samples; A) MS1; B) MS2; C) SIL	22
Figure 19 - RX-DD-A Digital Durometer	22
Figure 20 - Shore A Hardness measurement	22
Figure 21 - 2D drawing of compression mold	23
Figure 22 - SIL sample dispensed	23
Figure 23 - Eco-duo 330 dispenser.....	23
Figure 24 - Compression test (load and unload)	23
Figure 25 - A) MS1 compression test; B) ZW-S7040 (Omron) laser	24
Figure 26 - Lap shear tests methodologies.....	24
Figure 27 - Adhesive shear stress (adapted from [42])	25
Figure 28 -2D lap shear sample.....	25
Figure 29 - 2D Sample spacers, A) upper, b) lower	26

Figure 30 - 3D samples for each substrate (MG, PG and PC)	26
Figure 31 - A) MS1 cartridge; B) MS2 cartridge; C) SIL cartridge; D) Double side tape	26
Figure 32 - Pneumatic dispenser	27
Figure 33 - Static mixers	27
Figure 34 - Lap shear machine	27
Figure 35 - Screwing load cell device	28
Figure 36 - Screwing load cells calibration.....	28
Figure 37 - 1 st screwing: 2 screws.....	29
Figure 38 - 2 nd screwing: 4 screws	29
Figure 39 - 3 rd screwing: 3 screws.....	29
Figure 40 - 4 th screwing: 3 screws	29
Figure 41 - Pallet movement in structural bonding cell	29
Figure 42 - Accelerometer device	30
Figure 43 - Pallet movement.....	30
Figure 44 - Pallet movement (X,Y,Z).....	30
Figure 45 - Linear fitting of Owrk model for the dispersive component ($\gamma L (1 + \cos\theta)2\gamma Ldisp$) vs. Linear fitting of Owrk model for the polar component ($\gamma LpolyLdisp$).....	31
Figure 46 – A) Polar and dispersive surface energy of MG, PG and PC, with surface pre-treatments; B) - Surface polarity of MG, PG and PC, with surface pre-treatments	33
Figure 47 - Water contact angles and diiodomethane contact angles on MG, PG, PC substrates and IPA and plasma surface treatments	34
Figure 48 - Shore A hardness vs. time for MS1, MS2 and SIL adhesives	35
Figure 49 - Load (N) vs. displacement (mm) graph for adhesive MS1, cured for different times: 30, 60 and 90 minutes	36
Figure 50 - Stress (MPa) vs. Strain (%) graph for MS1 adhesive, cured for different times: 30, 60 and 90 minutes	37
Figure 51 - Stress (MPa) vs. Strain (%) graph for MS2 adhesive, cured for different times: 30, 60 and 90 minutes	37
Figure 52 - Strength (MPa) vs. Strain (%) graph for SIL adhesive, cured for different times: 30, 60 and 90 minutes	37
Figure 53 - Strength (MPa) vs. Strain (%) graph for DST	37
Figure 54 - Compression strength (MPa) vs. strain (%) of MS1 (30, 60 and 90 minutes cure)	38
Figure 55 - Compression strength (MPa) vs. strain (%) of MS2 (30, 60 and 90 minutes cure)	38
Figure 56 - Compression strength (MPa) vs. strain (%) of SIL (30, 60 and 90 minutes cure)	38
Figure 57 - DST compression strength (MPa) vs. strain (%).....	38

Figure 58 - Linear regression from strength vs. strain plots for all adhesives	39
Figure 59 - Load vs. displacement plot for DST adhesive joints using IPA on PC as surface pre-treatment (#11 - #15)	40
Figure 60 - Average maximum load (N) vs. displacement (#1 - #15).....	41
Figure 61 - DST shear strength for all 3 substrates (MG, PG and PC)	41
Figure 62 - Maximum load (N) vs. curing time (min)for MS1, MS2 and SIL	43
Figure 63 - Shear strength (MPa) for different curing times (DST, MS1, MS2 and SIL).....	43
Figure 64 - MS2 maximum load (N) using IPA and plasma pre-treatments on magnesium substrate	45
Figure 65 - MS2 maximum load (N) using IPA and plasma pre-treatments on painted glass substrates	45
Figure 66 - MS2 maximum load (N) using IPA and plasma	46
Figure 67 - MS2 shear strength adhesive results over time (10 and 30 minutes) using IPA and plasma pre-treatments on polycarbonate substrate	47
Figure 68 - Visteon display lens	49
Figure 69 - Visteon display carrier	49
Figure 70 - Sample 1 screwing load (N) over time	49
Figure 71 - Sample 2 screwing load (N) over time	49
Figure 72 - Sample 3 screwing load (N) over time	49
Figure 73 - 2D Visteon display carrier	50
Figure 74 - Acceleration on X direction (#7 test)	52
Figure 75 - Acceleration on Y direction (#7 test)	52
Figure 76 - Acceleration on Z direction (#7 test)	52
Figure 77 - 2D Visteon display lens	53
Figure 78 - Linear regression of strength (MPa) vs. velocity (mm/s), to reduce the holding time to 30 minutes	55
Figure 79 - Acceleration data (X axis).....	56
Figure 80 - Acceleration results at different speed (120 mm/s, 175 mm/s and 230 mm/s)	56

List of Tables

Table 1 - MS1 details and full cured properties.....	9
Table 2 - MS2 details and full cured properties.....	9
Table 3 - SIL full cured properties.....	10
Table 4 - Surface free energy measurements.....	20
Table 5 - Surface tensions of water and diiodomethane [37].....	20
Table 6 - Lap shear specimen dimensions for all substrates (MG, PG and PC).....	26
Table 7 - Schematic table for lap shear tests methodologies.....	28
Table 8 - Contact angle measurements (virgin magnesium).....	31
Table 9 – Virgin magnesium SFE results (#1 - #5).....	32
Table 10 - Polar energy, dispersive energy and surface free energy results.....	32
Table 11 - Polar and dispersive contact angle measurements.....	33
Table 12 - Shore A hardness results for MS1, MS2 and SIL adhesives.....	35
Table 13 - Adhesives curing rate over time (h).....	36
Table 14 - Linear regression for all adhesives at different curing times (30, 60 and 90 minutes).....	39
Table 15 - Minimum curing time for MS1, MS2 and Sil to obtain DST slope benchmark.....	40
Table 16 - Average maximum load using magnesium substrate.....	41
Table 17 - Average maximum load using glass substrate.....	41
Table 18 - Average maximum load using polycarbonate substrate.....	41
Table 19 - 1 st Methodology failure modes.....	42
Table 20 -1 st Methodology DST shear strength results and failure modes.....	42
Table 21 - Shear Load (N) and shear strength (MPa) for all 4 adhesives using PC substrate and IPA as surface pre-treatment.....	43
Table 22 - Curing time estimation for three glues (MS1, MS2 and SIL).....	44
Table 23 - 2 nd Methodology failure modes.....	44
Table 24 - Shear load (N) and shear strength (MPa) over time for MS2 using MG, PG and PC substrates and IPA and plasma surface pre-treatments.....	46
Table 25 - 3 rd Methodology failure modes.....	48
Table 26 - Ok / Not ok.....	50
Table 27 - Minimum area to assure Visteon strain specification (15%).....	51
Table 28 - Minimum holding time before screwing process for all glues.....	51
Table 29 - Maximum acceleration (m/s ²) at different velocities (120 mm/s, 175 mm/s, 230 mm/s).....	53

Table 30 - Acceleration strength for different pallet velocities	54
Table 31 - Minimum holding time before pallet movement for all adhesives	54
Table 32 - Maximum pallet speed (mm/s) to reduce the holding time to 30 minutes	55

List of Symbols

A – contact area

a – acceleration

$disp$ - dispersive component

ε – strain

m – mass

θ – contact angle

P – applied load

pol - polar component

$StandDev$ – standard deviation

Tg – glass transition temperature

w - specimen width

W_{adh} – work of adhesion

γ_L – surface tension of the liquid phase

γ_S – surface energy of the solid phase

γ_{SL} – interfacial surface tension

List of Acronyms

1K – One Component
2K – Two Components
ABJ – Adhesive Bonded Joints
ADAS – Advanced Driver Assistance Systems
ASTM – American Society for Testing and Materials
BTC – Bonding Technical Centre
CA – Contact Angle
DIN – German Institute for Standardisation
DST – Double Side Tape
EN – European Norm
IPA – Isopropanol
ISO – International Organization for Standardization
MG – Magnesium
MS1 – Silane-modified 1
MS2 – Silane-modified 2
MSA – Mobile Surface Analyser
PC – Polycarbonate
PG – Painted Glass
PLA – Polylactic Acid
PSA – Pressure Sensitive Adhesives
PUR – Polyurethane
SAH – Shore A Hardness
SFE – Surface Free Energy
SIL – Silicone
UV – Ultraviolet

1. Introduction

1.1 Context

The first mention of an adhesive is from a British patent in 1754. The first structural adhesives appeared in the late 19th century, but only during the first world war, early 20th century, massive production of structural adhesives began. Structural adhesives have become alternative to other methods of joining similar and dissimilar materials. The main revolution in adhesives took place during World War II, used in aircraft industry. That was also when adhesive searching started to be collected [1].

Today, it is impossible to think of a world without adhesives. In 2020 the global structural adhesives market was valued at approximately €14.3 billion. The market decreased in 2020 due to covid-19, but the global market is expected to grow to €27.9 billion in 2030, growing at a compound annual growth rate (CAGR) of 6.9% from 2021 to 2030 (Figure 1) [2].

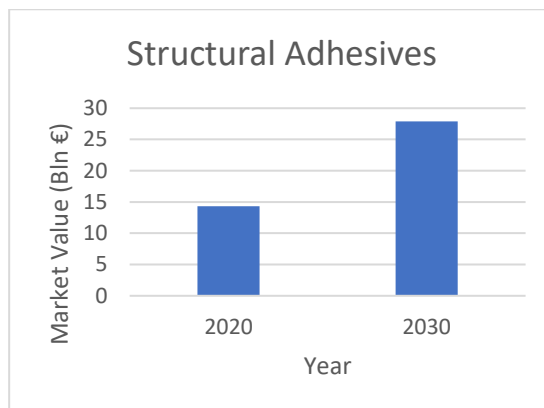


Figure 1 - Structural adhesives market value in 2020 and in 2030 (adapted from [2])

Mechanical joints, such as bolting, pinning, fastening, welding, or riveting, have a lot of use because it is quite simple and are suitable when disassembly is required. However, holes in mechanical joints result in micro and/or local damage during the manufacturing process, especially in composite materials, which consequently result in damage of the structure strength [3].

Adhesive bonding shows some advantages over mechanical joining methods. Adhesive bonded structures are very light and can be relatively cheap to manufacture. Show smooth stress distribution along the bonded length which translates into higher fatigue resistance. The ability to effectively join dissimilar materials is perhaps one of the most important advantages as it allows

the use of lightweight materials, such as composites that cannot be joined using other conventional methods. Adhesive bonding limitations are related to relative low peel strength, operational temperature limit and delayed production because of curing time [3-4].

Adhesive joints are used in many industries, such as automotive, aerospace, marine, and electronics, as they are more suitable in many aspects such as high strength to weight ratio, design flexibility, damage tolerance and fatigue resistance. The application of adhesive joints in the automotive industry has been increasing significantly in recent years, due to its potential for lighter vehicles, fuel reduction and emissions reduction [3].

1.2 Visteon

This dissertation topic was initially proposed by Visteon, an automotive electronics company. Visteon produce digital instrument clusters, displays, Android-based infotainment systems, domain controllers, advanced driver assistance systems (ADAS) and battery management systems (Figure 2). Company is headquartered in Van Buren Township, Michigan, and has more than 40 facilities in 18 countries, one of them in Palmela (Portugal).



Figure 2 - Visteon display product [5]

Adhesives, in digital instrument clusters and displays, have become more and more used to obtain lighter and cheaper products. Due to adhesive bonding importance, Visteon has founded the Bonding Technology Centre (BTC) in Palmela. BTC has the purpose of researching and testing of adhesives and the development of new bonding technology.

1.3 Display Assembly Process

In Visteon display manufacturing, during the assembly, there are two main bonding processes: optical bonding and structural bonding. This first pre-assembly is bonded to the metal carrier using structural adhesives, originating structural pre-assembly. Structural adhesive

bonding is one of the most popular methods of joining similar and dissimilar materials, which establishes strong physical bond between the two parts (Figure 3).

Clipping and screwing processes are used in the final assembly.

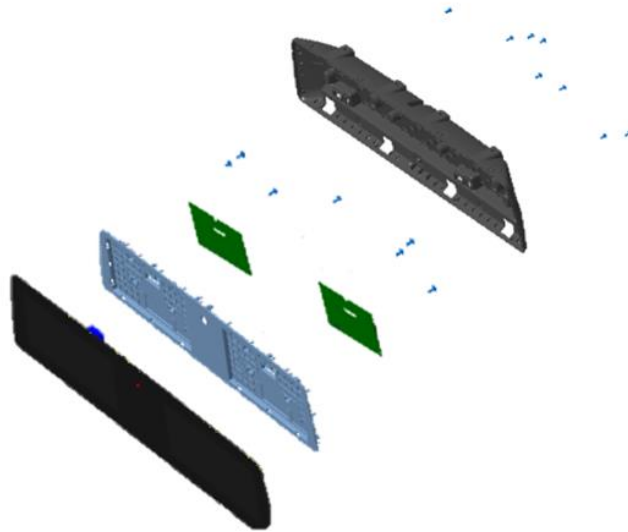


Figure 3 - Display assembly exploded view

It is very important to reduce the holding time between assembly processes. Using Figure 4 as an example, it would be necessary to create a buffer of 60 parts for each hour of curing time if a part is produced every 60 seconds (cycle time). The higher the adhesive curing time, the higher the holding time, the higher the buffer. Visteon's main goal is to define which glues does not need 90 minutes of buffer time between assembly processes.

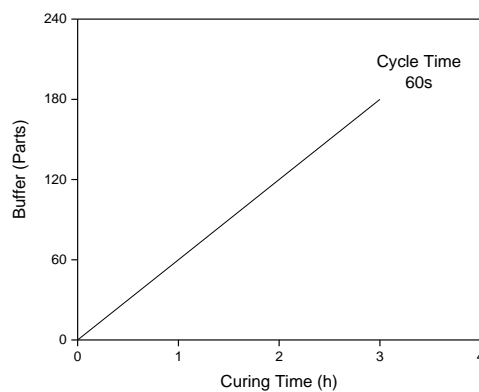


Figure 4 – Buffer (parts) vs. curing time (h)

1.3.1 Structural Bonding

This dissertation focusses only on structural adhesives and structural bonding process. Structural bonding process can be divided into three stages:

- **Surface treatment application**, plasma application to both parts, lens and carrier;
- **Structural glue dispensing**, glue dispensing on one of the parts;
- **Bonding**, bonding the lens to the carrier.

A pallet carries both parts, optical pre-assembly and carrier, moving forward and stopping at each station in a continuous cell.

1.3.2 Assembly Process Forces

Adhesives cannot delaminate at any time. They must resist during the manufacturing as well as its products life.

There are two main forces applied on the adhesives during the assembly process: shear forces and compression forces. Shear forces occur particularly on moving and stopping of the pallet along the cell, while compressive forces occur mainly when clipping and screwing parts on the final assembly.

1.4 Motivation and Objectives

The main motivation for performing this thesis was to carry out theoretical and practical research about a real problem in the automotive industry. All theoretical research on the bonding phenomena was important, but also all practical skills developed to solve engineering problems and implement solutions in a real environment.

The main goal of this dissertation was to find the best mechanically performing adhesive at the assembly process of a digital display. To do so, it was necessary to characterize different adhesive joints (adhesives and substrates) and resultant forces from the assembly process.

The thesis is divided into 6 chapters:

Chapter 1 – Introduction, presents the contextualization of this dissertation, the proposed objectives and the main contents of each chapter;

Chapter 2 – State of the Art, is where literature on adhesives is presented, followed by a review of adhesive joints, wettability and surface pre-treatments;

Chapter 3 – Material and Methodology. This chapter presents the materials, methodologies for substrates characterization (surface free energy measurements), adhesive characterization (shore A hardness, compression tests and lap shear tests) and process characterization (screwing forces and acceleration forces).

Chapter 4 – Results and Discussion, presents the results and discussion of surface characterization of 3 different substrates, using two different surface pre-treatments. It also presents results and discussion from the study of the curing time and the mechanical behavior of 4 adhesives. And is where the acceleration forces and the forces resulting from the screwing process have been characterized. Furthermore, using a real Visteon display as an example, it was estimated the minimum curing time before both assembly processes.

Chapter 6 – Conclusions, presents a summary of the results and the final conclusions, along with some considerations on further developments.

2. State of the Art

2.1 Adhesives

Adhesives are the substance that fills the gap between the materials to be bonded. When adhesives solidify, create a bond between the substrates. The scope of this section is characterizing the main types of adhesives available on the market. Adhesives can be divided into five classification methods: molecular structure, chemical composition, physical form, mechanical performance, and hardening method [6].

2.1.1 Molecular structure

As polymers, adhesives consist of long molecules, composed of many repeating molecular units. They result from polymerization processes which join the monomers into polymer chains. Polymeric materials have three types of distinct molecular structures, as shown in Figure 5, thermosetting polymers, thermoplastics, and elastomers [7].

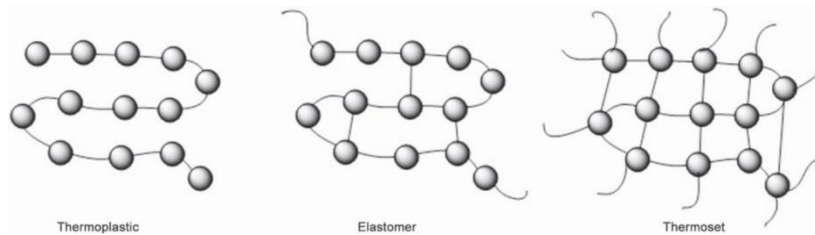


Figure 5 - Thermoplastic, elastomer, and thermoset molecular structures [8]

Thermosetting polymers have compact polymer chains, which have many chemical covalent bonds (cross-links), linking together the polymer chains. Thermosetting polymers do not melt, which means they can be operated at high temperatures without losing mechanical properties. any damage occurring. Most adhesive joints use thermosetting adhesives because of their mechanical strength and high durability [7].

Thermoplastics have a much more open molecular structure, with free polymer chains. A consequence of this freedom is that thermoplastic polymers melt after a certain temperature. They are therefore more flexible than thermosets and have a lower mechanical strength [7].

Elastomers consists of long polymeric chains, interconnected only by widely spaced covalent bonds. This results in a very flexible polymer, with high elastic recovery (resilience) [7].

2.1.2 Physical Form

The physical form of an adhesive is an aspect to consider in the adhesive selection process. The physical form of the adhesives can vary between liquid adhesives, pastes, films and tapes. Tape and paste adhesive are the most used in the automotive industry [9].

2.1.3 Mechanical performance

Adhesives can be categorized as structural or non-structural. Structural adhesives typically have mechanical strength higher than 7 MPa. High strength adhesives can even achieve tensile strengths of 40 MPa. A structural adhesive has the main function of supporting loads. Below 7 MPa, adhesives are called non-structural or sealants and, they have the function of sealing liquids or gases [10].

2.1.4 Curing Method

Curing method is the method by which the adhesive becomes solid enough to withstand service load. This process not always need a phase transition, as is the case of PSA (Pressure sensitive adhesives), which are activated by pressure [11].

Curing by chemical reaction

Many adhesives are made up of two components (2k), the resin (main component) and the hardener (chemical reagent). The reaction of the two components leads to establishment of cross-links, usually an exothermic reaction, and to the increase in molecular weight. There are also adhesives whose two components are already mixed in a single cartridge (one component adhesives, 1K). The chemical process is accelerated by heat. These adhesives ideally should be stored at low temperatures.

There are other types of one component adhesives that cure when exposed to ultraviolet light. UV light provides the energy needed to start the crosslinking process. In addition to UV light, there are also adhesives that harden with visible light, or electron beam [6].

Curing by physical processes

Many adhesives are supplied in the form of a liquid solvent, such as water, typically a dispersion of polymer particles in the solvent. After application, these adhesives must be exposed to a heat source for solvent to evaporate. The use of these adhesives is increasingly sought after as it reduces exposure to health hazards and associated pollution.

Hot melt adhesives, or also known as “hot melts”, are also implemented through a physical process. When heated up to a temperature above the melting temperature, they wet the surface to adhere and once the heat is removed, they solidify [6,11].

2.1.5 Chemical Composition

The chemical composition of an adhesive is related to the main polymeric chemical structure in the adhesive formulation. It is the most common way for manufacturers to classify adhesives. However, it is important to note that adhesives with the same chemical base can have very different properties [3].

Epoxies

Epoxies are typically highly cross-linked thermosets and, therefore, relatively strong, and stiff materials, with extensive use in structural applications. Epoxy adhesives cure exothermically and are dimensionally stable, with a relatively low curing shrinkage level. Epoxy adhesives can be supplied on one or two components. To prevent brittleness, epoxies can be reinforced with a tenacious material. Epoxy-polyurethane hybrid adhesives are very popular in the automotive industry because they combined high mechanical strength and toughness/ductility [3].

Polyurethanes

Polyurethanes are available in one or two-component formulations. One component polyurethane, 1K PUR, has higher flexibility and hardens with atmospheric vapor. Consequently, they cure very slowly and very dependent on air moisture. High temperatures can accelerate the curing process. In contrast, 2K polyurethanes are preferably used in structural applications because they have high resistance to both shear and pull-out loads. The two-component formulation gives them a very fast curing and no need for the application of heat or moisture [12].

One of the adhesives characterized in this study is a polyurethane-based adhesive (**MS1**). Silane end-capped urethane polymers undergo crosslinking reactions in the presence of catalyst and moisture to form a stable siloxane linked network. Its high-performance hybrid technology is a result of the synergy between the silane-curing mechanism and polyurethane backbone properties. Silane-modified polyurethanes generally exhibit better physical properties compared to conventional polyurethane adhesives [12].

MS1 is a one component polyurethane-based adhesive, whose cure can be promoted by using a 2nd component, a moisture booster in the (10:1 ratio). MS1 backbone is terminated by silane groups, which are supported by urethane groups. Silane-modified polyurethane (A-component) starts curing with ambient moisture and skinning effect can inhibit the curing of the adhesive in the centre of the bead as the bead reacts with ambient moisture. On the other hand, in a two-component system with the moisture booster (B-component) the cure is accelerated as the moisture is already distributed in all beads, centre included [14].

The technical specifications of **MS1** are presented in Table 1.

Table 1 - MS1 details and full cured properties

	Units	MS1	Observations
Base		Polyurethane	
Mixing Ratio		10:1	A:B
Component A		Silane polyurethane	Resin
Component B		Moisture Booster	Catalyst
Cure		Moisture Cure	Cure at room temperature (from +5°C to +40°)
Consistency		Pasty	
Pot Life	min	8	
Open Time	min	5	
Shore A Hardness		51	
Tensile Strength	MPa	2	DIN EN ISO 527
Shear Strength	MPa	3	DIN EN 1465
Glass Transition Temperature	°C	< -50	DMTA

Polyethers

Silane terminated polyether adhesives, also known as MS polymers, is one of the adhesives characterized in this research (MS2). MS polymer is silane terminated polyether prepared from high molecular weight polypropylene oxide. It is end capped with allyl groups, followed by hydrosilylation to produce a polyether end capped with methyldimethoxysilane groups. The water reacts with the methoxysilane group to liberate methanol and produce a silanol. Silanol reactions produces siloxane linkages [9]. The technical specifications of MS2 are presented in Table 2.

Table 2 - MS2 details and full cured properties

	Units	MS2	Observations
Base		Polyether	
Mixing Ratio		10:1	A:B
Component A		Silane polyether	Resin
Component B		Moisture Booster	Catalyst
Cure		Moisture Cure	Cure at ambient temperature (above 5°C)
Consistency		Pasty, Thixotropic	
Pot Life	min	2	
Open Time	min	4-5	
Shore A Hardness		55	ISO 868
Tensile Strength	MPa	3	ISO 37
Shear Strength	MPa	2	DIN EN 1465
Glass Transition Temperature	°C	< -50	

MS2 is silane-modified polyether (A component) which cures through polycondensation, also known as moisture curing, in room temperature. This polymer is similar to MS1, the change being the based-backbone polyether vs polyurethane-based, but the curing occurs in the same way.

Silicones

Silicone adhesives are available as 1K or 2K. These systems cure through polycondensation and/or radical polymerization. Silicone adhesives have low shear properties but excellent peel strength [14].

The third characterized adhesive in this research is a silicone-based adhesive (**SIL**). Silicone adhesives are based on mixtures of silicone-based polymers, crosslinking components, and catalysts. The studied silicone has a polydimethylsiloxane main chain with vinyl groups and SiH moieties for hydrosilylation, through a radical process. Functional silanes are used as crosslinking agents, in the presence of organometallic catalysts [14]. The technical specifications of **SIL** are presented in Table 3.

Table 3 - **SIL** full cured properties

	Units	SIL	Observations
Base		Silicone	
Mixing Ratio		10:1	A:B
Component A		Polydimethylsiloxane	Resin
Component B		Organometallic Platinum	Catalyst
Cure		UV Activation / Moisture Cure	10 seconds with a minimum exposure of 120 mW/cm ²
Consistency		Pasty	
Pot Life	min	10	
Open Time	min	1	
Shore A Hardness		30	
Tensile Strength	MPa	3	ISO 37
Shear Strength	MPa	1	
Glass Transition Temperature	°C	< -110	

SIL is a two-component silicone-based adhesive. The resin component (A component) is polydimethylsiloxane polymer with vinyl and SiH moieties for hydrosilylation. And B component is polydimethylsiloxane (vinyl) with platinum organometallic catalyst (ppm). Two components should be thoroughly mixed at a 10:1 ratio.

UV activates the platinum organometallic catalyst which through a platinum-catalysed hydrosilylation (radical process) creates the network links to form the silicone adhesive structure. This reaction takes place at room temperature.

The ideal conditions for curing **SIL** is 10 seconds with a minimum exposure of 120 mW/cm². In our study all samples with **SIL** were positioned for 10 seconds at 101.6 mm distance from the UV light which provides a power density of 145 mW/cm² to the adhesive.

Acrylics

Acrylic-based adhesives, although not as strong and rigid as epoxies, are very used in structural applications due to their extremely fast curing, which can speed up the production

processes of bonded components. The last of 4 adhesives studied is an acrylic-based adhesive with a foam core. Polyacrylate elastomers are used to make high performance pressure sensitive adhesives [15].

DST is an acrylic double side tape is an adhesive very used in industry, which does not require cure, only pressure. DST does not change mechanical properties over time and so it is a good benchmark for this research mechanical tests.

2.2 Adhesion Theory

An adhesive bonding process begins with an adhesive application process. When an adhesive it cures, creates a bond between the substrates, which after bonding are called adherents. An interface is formed between the adhesive and adherend surfaces. To occur adhesion, it is necessary to make a correct preparation of the substrates, ensuring good molecular contact along the interface, so that a perfect bond occurs, avoiding premature failures [16].

2.2.1 Adhesive Bonded Joints

There are several types of adhesive bonded joints (ABJ), already designed for different types of applications. Examples of the most common geometries are summarized in Figure 6.

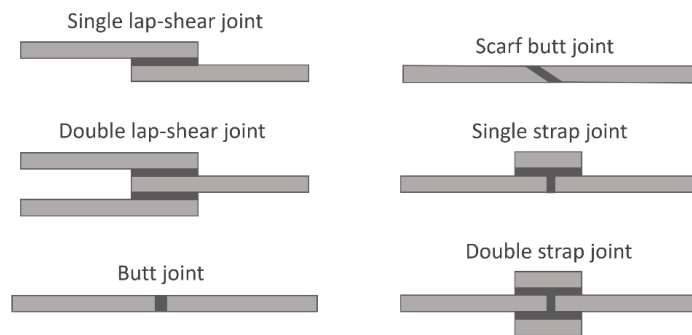


Figure 6 - Common adhesive joints [17]

The single lap-shear joint is the most common due to its simplicity and effectiveness. Chosen geometry must account all loading scenarios [18].

2.2.2 Loading Modes

Adhesive joints can have different types of design, supporting different types of loads. An adhesive joint provides a viable alternative to classical joining methods. The five main loading

modes of an adhesive joint are: tensile, compressive, shear cleavage and peel (Figure 7). The focus of this research will be on the compression and tensile-shear loading.

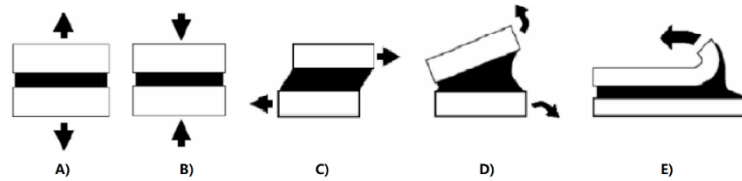


Figure 7 - Basic loading experienced by adhesive, A) tensile, B) compression, C) tensile-shear, D) cleavage, E) peel (adapted from [19])

In shear load condition, the adhesive layer is relatively well aligned with the load direction. In this load condition, adhesive withstand a greater load and have greater strength.

Adhesive bonds exhibit low resistance to both cleavage and peeling. Cleavage occurs when the load is concentrated on one end of the joint, while the opposite side remains almost unstressed. Most structural adhesives offer limited strengths under prying loads, which concentrates the acting load in a very small area. This leads to premature failure of the adhesive [20].

2.2.3 Adhesion forces

The main goal of ABJ is resist the external forces applied. Chemistry behind the adhesives and adherends is the first step to understand the mechanical behavior of adhesively bonded joints.

Adhesive bonds to adherents through chemical bonds and the type of adhesive forces depends on chemical nature of the surface material. There are two major adhesive forces: primary chemical bonding (more energetic), and secondary physical bonding (less energetic) [21].

In primary bonds, there is sharing or transfer of electrons between the atoms involved, which includes ionic, covalent, and metallic bonds. These are very strong bonds, however they are only effective at a few angstroms distance. In contrast, secondary bonds, van der Waals forces and hydrogen bonds, depend on the interaction between atomic and molecular dipoles [21].

2.2.4 Mechanisms of Adhesion

The adhesion phenomena have been the subject of several investigations, which resulted in several models and theories to explain its existence. However, there are no complete theories that are versatile enough to describe all the phenomena. Mechanical interlocking, physical adsorption and chemical bonding models are summarized:

Mechanical Interlocking. In this mechanical theory, adhesion occurs if there are certain types of irregularities, resulting from roughness or porosity, which act as hooks to prevent separation of the adherends. Mechanical interlocking process occurs when a liquid adhesive penetrates and fills all cavities and irregularities in the substrate and subsequently solidifies, preventing separation, Figure 8 [22].

Physical Adsorption. According to the adsorption theory, adhesion is the result of the binding forces that are generated when the molecules of the adhesive and substrate are brought into contact. In a physical adsorption process, the bond is created essentially by Van der Waals forces, Figure 8. To be effective, it is necessary to ensure good wettability, to bring many adhesive molecules close to the substrate surface [22].

Chemical bonding. This mechanism is similar to physical adsorption. Chemical bonding requires establishment of primary chemical bonds, between the atoms of the adhesive and the substrate. These types of bonds are extremely strong and contribute significantly to a high level of adherence [22] (Figure 8).

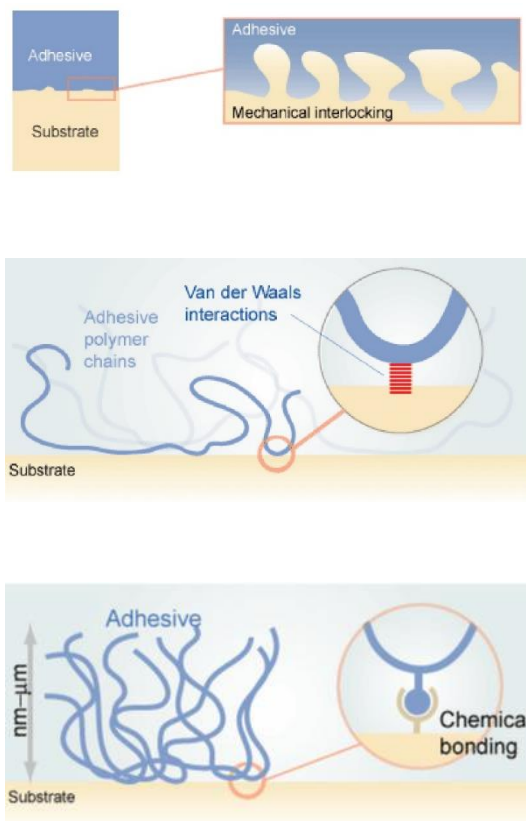


Figure 8 – A - Mechanical interlocking theory [23]; B - Physical adsorption theory (adapted from [29]); C - Chemical bonding theory (adapted from [24])

2.2.5 Failure Modes

There are three main failure modes, defined by the location of the own failure in the joint. They are adhesive failure, cohesive failure, and substrate failure (Figure 9).

Adhesive failure happens at the interface of one of the adherents. After breaking, one of the surfaces is completely covered with adhesive while the other contains only adhesive residues [25].

In cohesive failure mode, the adhesive reaches its load limit. This type of rupture occurs when the bond between the adhesive and the adherent is stronger than the internal strength of the adhesive itself [25].

In adhesive joint design, the optimal design is when the failure occurs in one of the substrates, which shows that the adhesive joint is stronger than the adherend material [25].

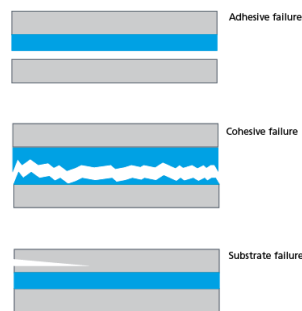


Figure 9 - Adhesive failure modes [26]

2.3 Wettability

Liquid adhesives, in an ideal scenario would completely wet all surface substrate. But usually, adhesives are repelled by the surface. Adhesive's ability to wet and spread spontaneously on the substrate surface has a real impact on ABJ [27].

2.3.1 Contact Angle

A contact angle (θ) is formed between the solid surface and the line tangent to the edge of the liquid drop, which results in a quantitative measure of the surface wettability of a liquid. This angle has a lower limit of 0 degrees, indicating that the liquid is either completely wetting the surface, and an upper limit of 180 degrees, indicating that the liquid does not wet the surface (Figure 10) [28].

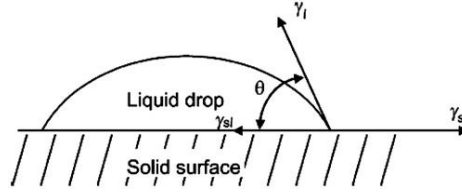


Figure 10 - Surface-wetting characterization using contact angle measurements [29]

2.3.2 Surface Free Energy

Wettability degree is determined by a balance of forces between the adhesive and the cohesive forces. All molecules in a bulk liquid are surrounded in all directions by other molecules, and so equally attracted. There are only cohesive forces. But when the liquid adhesive is in contact with the surface, there is only cohesive forces adjacent and below surface molecules, which promotes an excess of surface energy. Surface energy is the work that would be supplied to bring the molecules from the bulk material to its surface to create a new surface energy. Liquid tends to form minimal surface free energy such as round droplets.

Work of adhesion, W_{adh} , is defined as the thermodynamic work required to separate the interface from the equilibrium state of two phases [29, 30].

$$W_{adh} = \gamma_L + \gamma_S - \gamma_{SL} \quad (1)$$

γ_L is surface tension of a liquid phase, γ_S is the surface energy of the solid phase and γ_{SL} interfacial surface tension. When applied to the physical situation of a liquid drop on a solid surface, the concept of work of adhesion combined with Young's law produces the Young–Dupré equation:

$$\gamma_S = \gamma_{SL} + \gamma_L \cdot \cos\theta \quad (2)$$

$$\cos\theta = \frac{(\gamma_S - \gamma_{SL})}{\gamma_L} \quad (3)$$

$$W_{adh} = \gamma_L + \gamma_L \cdot \cos\theta \quad (4)$$

$$W_{adh} = \gamma_L(1 + \cos\theta) \quad (5)$$

The surface energy could be calculated, in terms of dispersive and polar or non-dispersive components, using the geometric mean equation combined with Young's equation.

$$\gamma_L(1 + \cos\theta) = 2 (\gamma_S^{disp} \gamma_L^{disp})^{1/2} + 2 (\gamma_S^{pol} \gamma_L^{pol})^{1/2} \quad (6)$$

where *disp* and *pol* represent the dispersive and polar components, respectively [28].

2.4 Surface Preparation

Surface preparation is a key process to create a strong, long-lasting adhesive joint, as it dramatically affects the level of adhesion between the adhesive and the substrate and consequently to control the strength of the joint. Incorrect surface preparation results in a joint with a low load bearing capacity [31].

The main goal is to optimize the adhesion forces between the substrate surface and the adhesive layer. It must be a compromise between surface wettability, adhesive viscosity, and substrate roughness [32].

2.4.1 Surface Preparation Selection

To select the surface treatment, it is necessary to know the main physical and chemical characteristics of the selected materials. Treatment chosen significantly influences mechanical behavior, as well as the durability of the adhesive joints.

The surface treatment of metals depends on several factors, the most important being the oxide layer on the surface. In metals, there are stable oxides strongly bound to the base materials and oxides that are found in layers with low mechanical strength. It is appropriate to remove them and replace them with a stable and well-controlled oxide. Ideally, surface preparation should remove all surface layers until the base metal is exposed.

Polymers naturally have low surface energy and exhibit very dynamic surfaces. They continually establish new internal balances with the interior of the polymer and external balances with the environment. Contaminants can be found on surfaces, such as plasticizers, release agents, lubricant, or simply contaminated by handling.

Composites have properties inherent to each constituent. In structural applications, adhesive bonds are almost always chosen technique, as it does not require drilling or other modifications. It is common to find release agents, resulting from their manufacturing processes. It is advisable to clean it and do not use intensive abrasive treatments to avoid damage to the surface [9, 33].

2.4.2 Pre-treatment Process

There are two major groups in surface treatment: passive treatments and active treatments.

Passive Treatments

In passive treatments, there is no change in the chemical nature of the adherent surface. Generally, these passive treatments are only an initial process, which do not dispense an active treatment.

Chemical cleaning is a passive surface treatment, which aims to remove greasy areas. Degreasing results in a clean surface by increasing surface free energy, improving the wettability of the adhesives. This process can be implemented through manual cleaning, immersion, spraying, steaming or exposure to ultrasound. Polar agents dissolve polar contaminants and non-polar agents perform best on surfaces with non-polar contaminants [33].

Active Treatments

Active treatments are used for cleaning and removing weak layers, changing the chemical nature of the surface. In metals, weak layers and oxide layers are removed, leading to an improvement in mechanical adhesion. In plasma treatment, the surface chemistry of the polymer is changed.

Plasma consists of a mass of air that has been subjected to a strong electrical discharge, which causes the dissociation of the molecular bonds of its constituent gases, transforming it into a plasma containing charged particles of electrons and positive ions that react easily with materials. Most polymers have chemically inert, non-porous surfaces [34].

3. Materials and Methodology

3.1 Substrate Characterization

3.1.1 Surface Free Energy

3.1.1.1 Principles

There are different methods to calculate surface free energy. Both, Owrk method and Zu method, divide the surface free energy into polar and dispersive components. However, Owrk method is the most used and it was chosen to calculate the surface free energy (SFE) of the three substrates of this study because it has an emphasis on the geometric interaction [33]. According to Young's equation, contact angle results (Figure 11) from a force equilibrium (Equation 7).

$$\cos\theta = \frac{(\gamma_S - \gamma_{SL})}{\gamma_L} \quad (7)$$

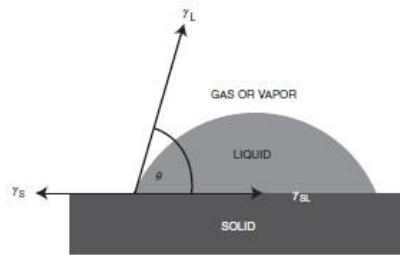


Figure 11 - Contact angle (θ) [36]

Based on this approach and using Fowke's relation, Owrk model leads to Equation 8:

$$\gamma_{SL} = \gamma_S + \gamma_L - 2\left(\sqrt{\gamma_S^d \gamma_L^d} + \sqrt{\gamma_S^p \gamma_L^p}\right) \quad (8)$$

, where γ_L^d and γ_L^p represent the dispersive and polar parts of the liquid respectively, while γ_S^d and γ_S^p are the respective contributions of the solid. Substituting Equation 8 into Equation 9:

$$\frac{\gamma_L(1+\cos\theta)}{2\sqrt{\gamma_L^d}} = \sqrt{\gamma_S^p} \sqrt{\frac{\gamma_L^p}{\gamma_L^d}} + \sqrt{\gamma_S^d} \quad (9)$$

Owrk model enables to obtain each component of the SFE by means of a linear fitting of equation, by plotting $\frac{\gamma_L(1+\cos\theta)}{2\sqrt{\gamma_L^d}}$ versus $\sqrt{\frac{\gamma_L^p}{\gamma_L^d}}$ [33].

3.1.1.2 Materials

In this section three different substrate materials are studied, AZ91D magnesium alloy (MG), painted aluminosilicate glass (PG), and polycarbonate (PC) (Figure 12). Magnesium alloy and painted glass are materials used on displays manufacturing process. The glass is painted for aesthetic reasons. It has 3 acrylic-based layers, printed, and cured with UV light. Polycarbonate was chosen because it is not only cheaper and faster to obtain as samples for this thesis, but also for further investigations and feasibility studies.



Figure 12 - Substrates employed in this study: magnesium alloy, painted glass and polycarbonate

As seen in the previous chapter, surface preparation strongly affects the level of adhesion between the adhesive and the substrate, and therefore the load bearing capacity of the part. Surface free energy measurements were carried out in all three substrate materials.

3.1.1.3 Methodology

In this study, Surface free energy (SFE) measurements were tested on three substrates, magnesium (MG), painted glass (PG) and polycarbonate (PC) in three different treatment conditions:

- Virgin (not treated);
- Cleaned with isopropanol;
- Plasma treated.

2 μ l droplets of both, polar (water) and dispersive (diiodomethane) liquids, were deposited on the substrate and the contact angles were measured by the sessile drop method with a Mobile Surface Analyzer MSA (Krüss) equipment (Figure 13). Measurements were made at 25 \pm 1 $^{\circ}$ C and 50 \pm 5 % humidity.

All measurements are summarized in Table 4.

Table 4 - Surface free energy measurements

# SFE Measurement	Substrate	Surface Treatment
#1 - #5	Magnesium	None
#6 - #10		Isopropanol
#11 - #15		Plasma
#16 - #20	Painted Glass	None
#21 - #25		Isopropanol
#26 - #30		Plasma
#31 - #35	Polycarbonate	None
#36 - #40		Isopropanol
#41 - #45		Plasma

The two test liquids have different well-known liquid surface tensions (Table 5).

Table 5 - Surface tensions of water and diiodomethane [37]

Test Liquid	γ_L	γ_L^d	γ_L^p
Water	72.8	21.8	51
Diiodomethane	50.8	50.8	0

Plasma treatment was applied at 10 mm/s. Piezobrush PZ3 (TDK) plasma equipment (Figure 14) has two distinctive tips, a “Standard Module” and a “Nearfield Module” (Figure 15). “Standard Module” was applied on non-conductive materials, glass, and polycarbonate. “Nearfield Module” was used on magnesium, a conductive material.



Figure 13 - Mobile surface analyzer (Krüss) equipment

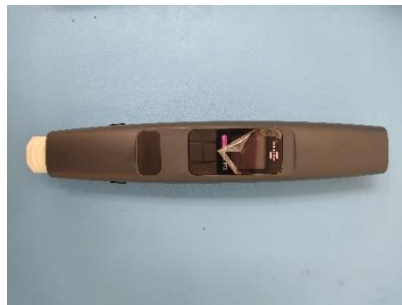


Figure 14 - Piezobrush PZ3 (TDK)



Figure 15 - Standard module and nearfield module

Visteon specifies that 50 mN/m is the minimum SFE in production and for this reason it is also this research SFE benchmark.

3.2 Adhesive Characterization

All adhesives MS1, MS2, SIL, and DST were tested. Substrate material has a great influence on adhesion, strength of the joint and on the failure mode of a particular joint. For this reason, three substrate materials specimens were chosen for the study, magnesium alloy, painted glass and polycarbonate.

3.2.1 Hardness Test

In this research hardness was used as an indicator of adhesive's curing. Commonly used hardness scales are Shore A - D. Shore A is used for soft materials, whereas Shore D is used for rigid materials (Figure 16). Adhesives hardness is typically measured by Shore A Hardness (SAH).

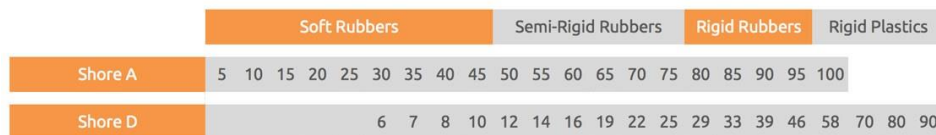


Figure 16 - Shore A and Shore D comparison (adapted from [38])

3.2.1.1 Principles

To characterize the hardness of adhesives, the industry typically uses the Shore A Hardness scale. Shore A indenter has an angle of 35° and a diameter of 0.79 mm. Lower hardness results from a greater penetration of the indenter in the sample. SAH of 0 results in an indentation of up to 2.5 mm, and SAH of 100 results in an indentation of 0 mm [39].

3.2.1.2 Materials and Specimen Preparation

The three glues, MS1, MS2, and SIL, were dispensed into a mold with 50mm x 20mm x 5mm dimensions. The mold was modelled (Figure 17), and 3D printed in PLA material (Figure 17).

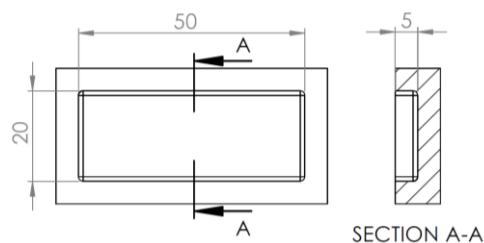


Figure 17 - 2D hardness sample mold

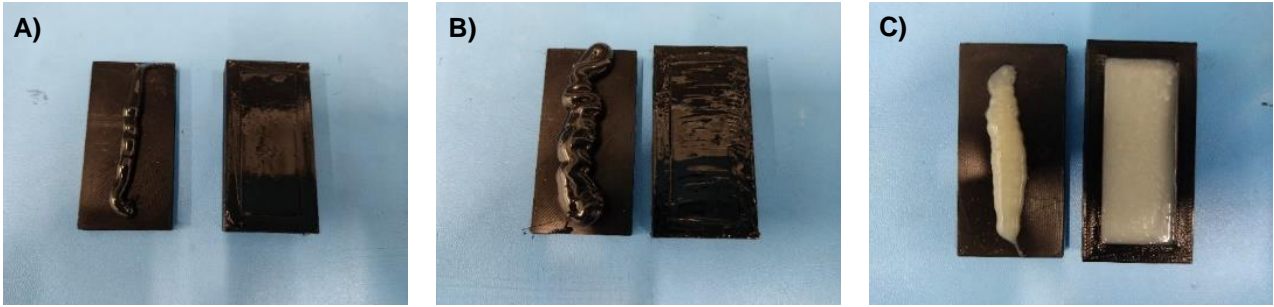


Figure 18 - Hardness samples; A) MS1; B) MS2; C) SIL

3.2.1.3 Methodology

The tests were performed under temperature-controlled conditions to the reference temperature of 22 °C. This method is based on the penetration of an indenter into the material surface. RX-DD-A Digital Durometer (Check-line), (Figure 19), was placed perpendicularly to the surface of the specimens (Figure 20). The hardness was measured as a function of curing time.



Figure 19 - RX-DD-A Digital Durometer

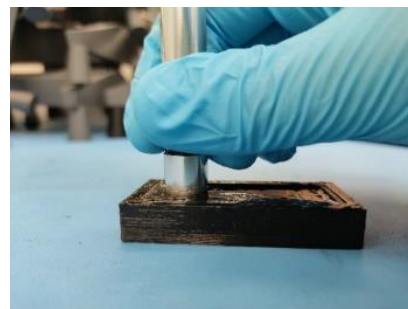


Figure 20 - Shore A Hardness measurement

Samples were tested after 30 min, 1h, 2h, 4h, 8h, 12h, 24h. The hardness measurements, for each specimen, resulted from five readings taken at five different positions on the surface. Measurements were taken at 9 mm away from the edges and least 6 mm distance from the indenter point, according to ISO 868 [40].

3.2.2 Compression Test

The main goal of these compression tests is to relate the compressive stresses of the adhesives to the maximum stresses applied when screwing on the final assembly process.

3.2.2.1 Principles

In compression tests, the forces involved tend to compress one adherent against the other, reducing the thickness of the adhesive. There is a constant distribution of stresses across the

adhesive. There is no standard for performing compression tests in adhesives. A compression test was developed to characterize the adhesive when compressed by the screwing processes.

3.2.2.2 Materials and Specimen Preparation

All four adhesives were used in the compression test: MS1, MS2, SIL and DST. In order to obtain the same adhesive area (1000 mm²), a mold was modelled, and 3D printed (Figure 21). The adhesives were dispensed along two straight lines (Figure 22), through the eco-duo 330 (Preeflow), a volumetric dispenser (Figure 23).

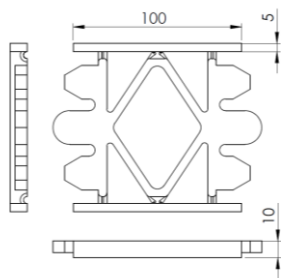


Figure 21 - 2D drawing of compression mold

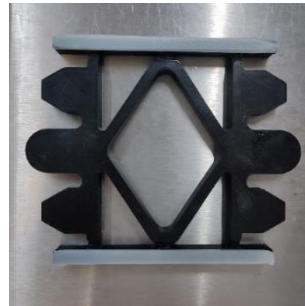


Figure 22 - SIL sample dispensed



Figure 23 - Eco-duo 330 dispenser

3.2.2.3 Methodology

After glue dispensing, the pieces were bonded to the glass with a spacing of 2mm between the mold and the glass. This distance was ensured by using spacers. When the adhesives reached the intended curing time for the test: 30, 60, and 90 minutes, the spacers were removed, and the sample was loaded and unloaded (Figure 24).

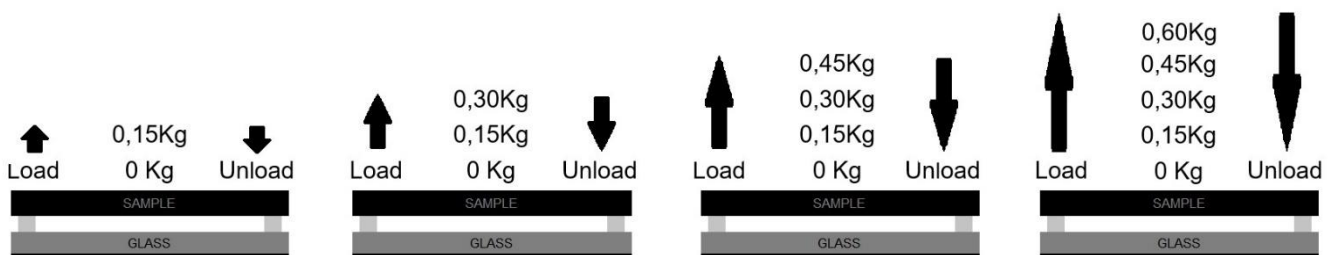


Figure 24 - Compression test (load and unload)

For each load applied on the sample, the displacement of the adhesive was obtained using ZW-S7040 (Omron) laser sensor equipment (Figure 25). Three samples were tested for each condition.

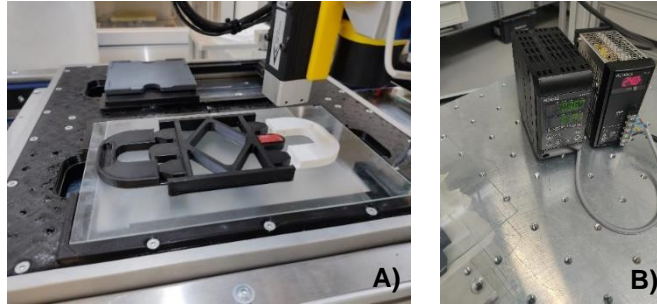


Figure 25 - A) MS1 compression test; B) ZW-S7040 (Omron) laser

Visteon does not have a defined specification for stiffness behavior in a non-fully cured state, and so for this trial it was agreed to use a strain metric. All glues were compared with the acrylic double side tape (DST) because it is an adhesive already used in Visteon products.

3.2.3 Lap Shear Test

The shear stresses for different adhesive joints, varying the adhesive, were calculated by lap shear tests, varying the adhesive, but also the substrate, the curing time, and the surface treatment applied to the substrate. By interest of time, as there was no time to do all combinations, the tests were divided into three methodologies, to characterize all variables (Figure 26). The adhesives and substrates for each methodology were chosen based on the results on the previous one. The first and second methodology two of the variables were kept constant, varying only the third one. In the third methodology only one variable was kept. After the tests, it was also intended to observe the failure mode of each sample.

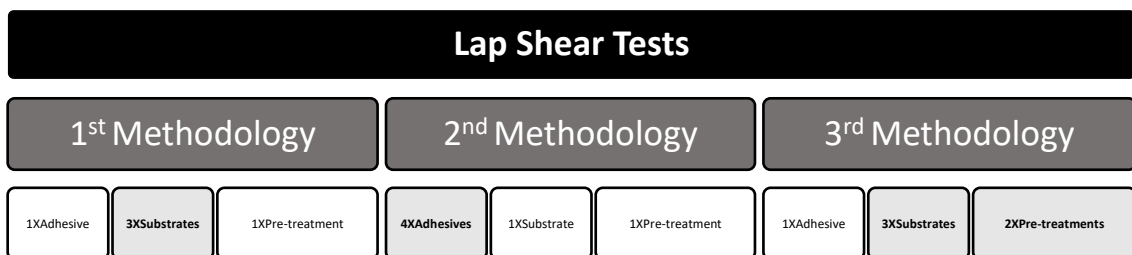


Figure 26 - Lap shear tests methodologies

In the first methodology only, one adhesive and one surface pre-treatment were tested. Acrylic double side tape (DST) was chosen because there was no required time for curing. Besides MG and PG, PC was also used as a substrate in the first methodology. For economic and logistical reasons, and due to the high number of specimens used, PC was the chosen substrate for the second methodology. The first methodology was mainly to understand if PC was a reasonable choice to be used as the reference substrate for the second methodology. In the second methodology, shear tests were performed varying the adhesives, but keeping the substrate and a single surface treatment. In the third methodology, lap shear tests were performed

using the better performing adhesive from the previous block, and now varying the substrate and surface pre-treatment.

3.2.3.1 Principles

Shear tests use two parallel but opposite loads, which cause a shearing effect on the material. The adherends are subjected to tensile stress, while the adhesive layer is subjected to shear stress, combined with pull out stress. Shear tests on simple overlap joints are very common, as the joints are simple and economical to manufacture, and these joints are also widely used in industry [41].

Shear tests are more relevant to adhesives than tensile tests. Most of the stress is localized at the ends of the overlap. The centre of the lap joint contributes little to joint strength. The stresses of a single lap joint specimen are shown in Figure 27. [41]

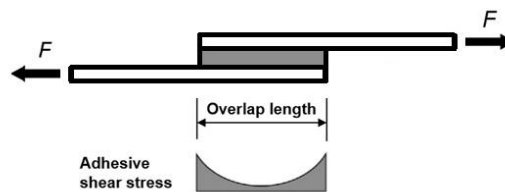


Figure 27 - Adhesive shear stress (adapted from [42])

3.2.3.2 Specimen Dimensions

All samples were 100 mm high and 25 mm wide, but the thickness of the samples has been deviated from the ISO 4587 [43] standard for logistical reasons (Figure 28). Magnesium specimens were 1.4mm thick, glass specimens 1 mm thick and polycarbonate were 1.4 mm thick (Table 6).

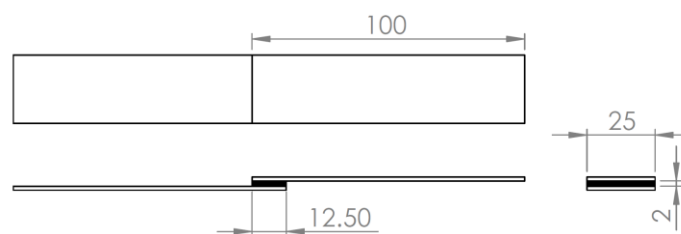


Figure 28 -2D lap shear sample

Table 6 - Lap shear specimen dimensions for all substrates (MG, PG and PC)

Substrate	Height (mm)	Width (mm)	Thick (mm)
Magnesium	100	25	1.4
Painted Glass	100	25	1.0
Polycarbonate	100	25	1.4

3.2.3.3 Specimen Preparation

To prepare the samples, two molds were designed and 3d printed. An upper part mold and a lower mold, (Figure 29, A and B, respectively). Once assembled (Figure 30), one substrate specimen settles on the lower mold and 312.5 mm² glue is dispensed onto the substrate. After dispensing, the second substrate settle on the upper mold, bonding the two substrates together and ensuring a glue height of 2mm. The bead height is defined by the difference in mold heights, which varies from substrate to substrate. The 2mm overlap height, is a deviation from the ISO 4587 standard, because it is the target height for Visteon products.

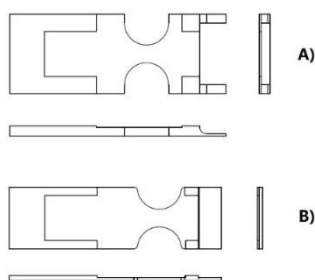


Figure 29 - 2D Sample spacers, A) upper, b) lower

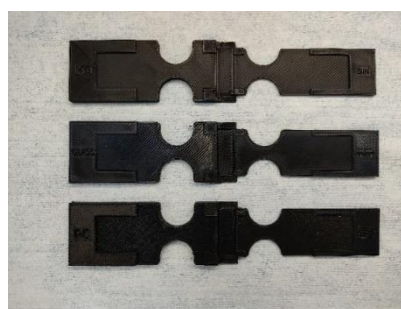


Figure 30 - 3D samples for each substrate (MG, PG and PC)

All three glues were supplied in 10:1 cartridges (adhesive: hardener ratio) (Figures 31). Dispensing was done using a pneumatic dispenser (Figure 32), and static mixers (Figure 33). Static mixers feature a helical geometry to force the two components to change direction and thus promoting the mixture.



Figure 31 - A) MS1 cartridge; B) MS2 cartridge; C) SIL cartridge; D) Double side tape



Figure 32 - Pneumatic dispenser

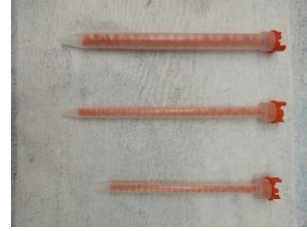


Figure 33 - Static mixers

As it has been mentioned in state of the art, surface treatment is very important during the bonding process because it is a crucial factor to ensure the quality of the adhesive bonding. Two types of surface treatment were used, isopropanol cleaning and plasma treatment.

3.2.3.4 Methodology

Lap shear test of the adhesive joints was performed on Instron 5566 universal testing machine, with the load-displacement data being collected using a 10 kN load cell. The tests were displacement controlled with a velocity of 3 mm/min. Tests were performed on all specimens, with the main objective of evaluating the shear strength of each joint. All experiment were performed at room temperature. There were two mandatory requirements to achieve good results: adhesive layer must not contain air bubbles, and the load should be applied in the plane of the adhesive (Figure 34).



Figure 34 - Lap shear machine

Lap Shear tests were divided into three methodologies to characterize all variables of these adhesive joints (Table 7):

Table 7 - Schematic table for lap shear tests methodologies

Methodology	#Sample	Adhesive	Substrate	Curing Time	Surface Treatment
1 st	#1 - #5	DST	MG	-	IPA
	#6 - #10		PG		
	#11 - #15		PC		
2 nd	#16 - #20	MS1	PC	30	IPA
	#21 - #25			60	
	#26 - #30			90	
	#31 - #35	MS2		30	
	#36 - #40			60	
	#41 - #45			90	
	#46 - #50	SIL		30	
	#51 - #55			60	
	#56 - #60			90	
3 rd	#61 - #65	MS2	MG	10	IPA
	#66 - #70				Plasma
	#71 - #75			30	IPA
	#76 - #80				Plasma
	#81 - #85		PG	10	IPA
	#86 - #90				Plasma
	#91 - #95			30	IPA
	#96 - #100				Plasma
	#101 - #105		PC	10	IPA
	#106 - #110				Plasma
	#31 - #35			30	IPA
	#111 - #115				Plasma

For all series samples, the failure mode of adhesive joints was determined visually.

3.3 Assembly Forces

3.3.1 Screwing Forces

Screwing process occurs after the structural bonding, in the final assembly.

3.3.1.1 Methodology

For screwing forces tests a five-load cell device was used (Figure 35), developed in Visteon, which could measure vertical forces (perpendicular to the load cells) applied to a product during screwing operations. After the equipment's calibration for different loading weights (Figure 36), automatic screwing test started.

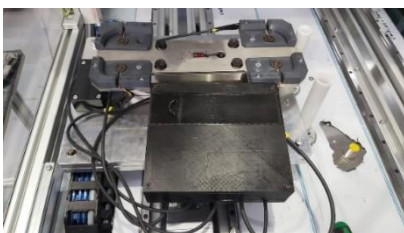


Figure 35 - Screwing load cell device



Figure 36 - Screwing load cells calibration

A total of 11 screws were screwed in each sample (Figures 37, 38, 39 and 40). All screwing and unscrewing operations take about 2 seconds per screw.



Figure 37 - 1st screwing: 2 screws

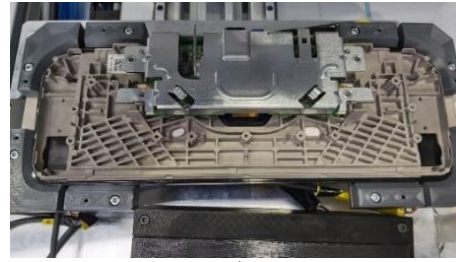


Figure 38 - 2nd screwing: 4 screws



Figure 39 - 3rd screwing: 3 screws



Figure 40 - 4th screwing: 3 screws

3.3.2 Acceleration Forces

All displays parts were positioned on a pallet. The pallet stops, and after each process the pallet restart moving forward to the next process. In this section, these acceleration forces are characterized, caused by the starting and stopping movements along the cell (Figure 41).

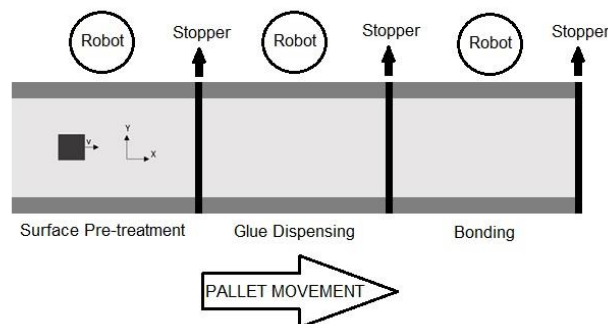


Figure 41 - Pallet movement in structural bonding cell

3.3.2.1 Methodology

Acceleration forces were measured by an accelerometer device (Figure 42), a method at Visteon, which was attached to a pallet. The pallet started moving in X direction (Figure 43) after stopper impact, down, delays a few seconds, then pallet ups and restarts moving forward again (Figure 44). The test was done with 3 different velocities, 120 mm/s, 175 mm/s, and 230 mm/s, each velocity was tested 3 times.

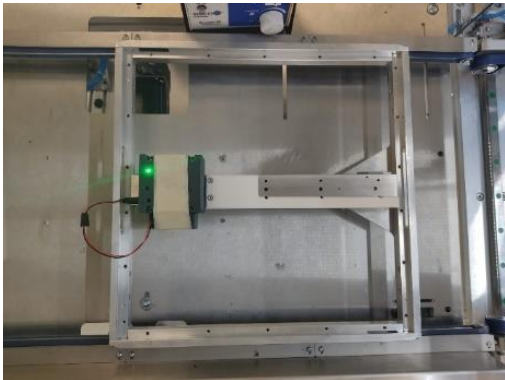


Figure 42 - Accelerometer device

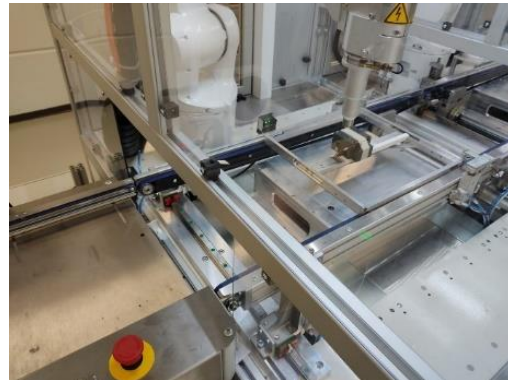


Figure 43 - Pallet movement

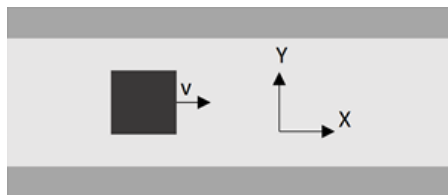


Figure 44 - Pallet movement (X,Y,Z)

4. Results and Discussion

4.1 Substrate Characterization

4.1.1 Surface Free Energy

Due to the high number of tests, a representative example of the first 5 measurements, calculations and graphics will be presented, and after that all test results will be summarized. Contact angles (θ) are the mean value from both sides. Contact angle measurements of magnesium without any treatment, are illustrated in Table 8.

Table 8 - Contact angle measurements (virgin magnesium)

	#1	#2	#3	#4	#5
θ^{disp} (°)					
θ^{pol} (°)					

It is possible to obtain SFE of the substrate using the Owrk method, by plotting $\frac{\gamma_L(1+\cos\theta)}{2\sqrt{\gamma_L^{disp}}}$

versus $\sqrt{\frac{\gamma_L^{pol}}{\gamma_L^{disp}}}$, Figure 45.

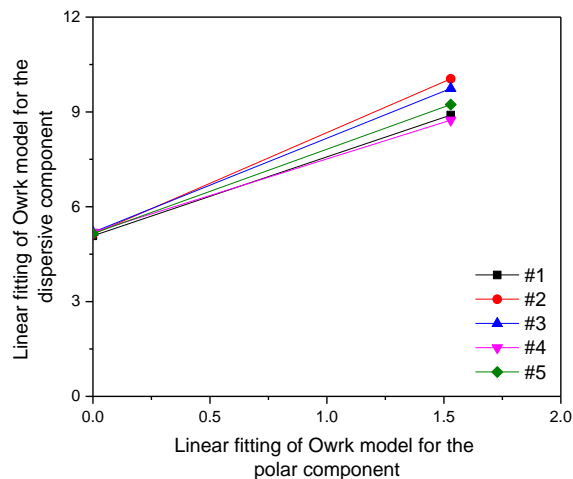


Figure 45 - Linear fitting of Owrk model for the dispersive component ($\frac{\gamma_L(1+\cos\theta)}{2\sqrt{\gamma_L^{disp}}}$) vs. Linear fitting

of Owrk model for the polar component ($\sqrt{\frac{\gamma_L^{pol}}{\gamma_L^{disp}}}$)

The polar component (γ_s^p) was obtained by the squares of the slope and the dispersive components (γ_s^d) by the squares of y-intercept. The value of SFE (γ_s) was determined as a sum of the two SFE components (Table 9):

Table 9 – Virgin magnesium SFE results (#1 - #5)

#Test	θ^d (°)	θ^p (°)	$\frac{\gamma_L(1+\cos\theta)}{2\sqrt{\gamma_L^d}}$	$\sqrt{\frac{\gamma_L^p}{\gamma_L^d}}$	γ_s^d	γ_s^p	γ_s
#1	64.81	81.85	2.50	5.08	6.24	25.81	32.05
#2	63.88	73.22	3.21	5.13	10.32	26.34	36.67
#3	62.76	75.55	2.97	5.19	8.84	26.99	35.82
#4	62.78	83.05	2.32	5.19	5.37	26.98	32.35
#5	63.55	79.37	2.67	5.15	7.13	26.53	33.66

Owrk model was used, and the mean results are presented in Table 10.

Table 10 - Polar energy, dispersive energy and surface free energy results

# Test	Substrate	Treatment	γ_s^{pol} (mN/m)	StandDev (mN/m)	γ_s^{disp} (mN/m)	StandDev (mN/m)	γ_s (mN/m)	StandDev (mN/m)	Surface Polarity (%)
#1 - #5	MG	None	7.580	± 1.999	26.532	± 0.491	34.112	± 2.065	22.22
#6 - #10		IPA	10.430	± 0.921	28.834	± 0.222	39.652	± 0.951	26.30
#11 - #15		Plasma	25.108	± 1.614	35.090	± 1.334	60.198	± 1.113	41.71
#16 - #20	PG	None	1.444	± 0.533	43.678	± 2.170	45.122	± 1.670	3.20
#21 - #25		IPA	6.022	± 2.031	39.016	± 0.785	45.038	± 1.355	13.37
#26 - #30		Plasma	24.884	± 1.461	42.064	± 0.314	66.948	± 1.532	37.17
#31 - #35	PC	None	2.558	± 0.399	42.218	± 1.775	44.776	± 1.714	5.71
#36 - #40		IPA	3.184	± 0.309	44.090	± 0.309	47.274	± 1.107	6.74
#41 - #45		Plasma	19.244	± 1.342	42.158	± 0.367	61.402	± 1.073	31.34

SFE summary:

IPA treatment: Magnesium (39.7 mN/m) < Painted Glass (45.0 mN/m) < Polycarbonate (47.3 mN/m)

Plasma treatment: Magnesium (60.2 mN/m) < Polycarbonate (61.4 mN/m) < Painted Glass (66.9 mN/m)

It is evident that, both surface pre-treatment mainly increased the polar component of each substrate, especially plasma surface pre-treatment (Figure 46). Plasma pre-treatment increases the polar surface free energy, as the concentration of polar groups increases [34].

Visteon benchmark (50 mN/m) was only achieved when using plasma pre-treatment.

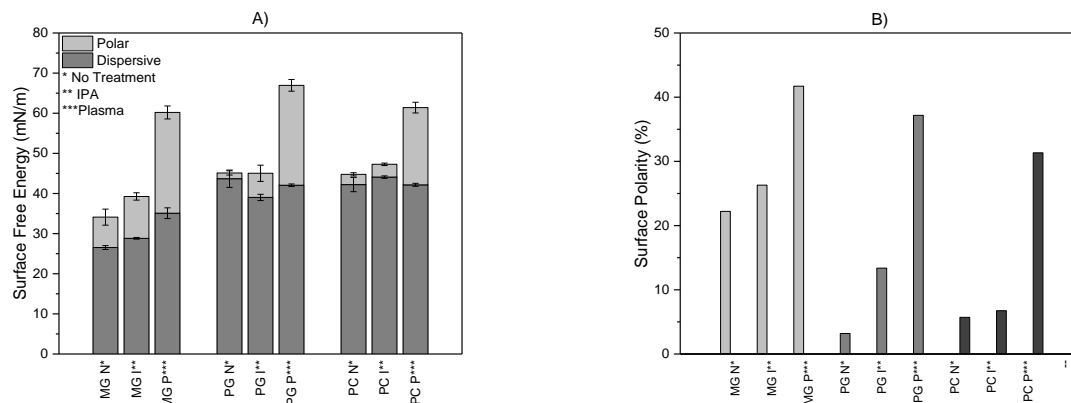


Figure 46 – A) Polar and dispersive surface energy of MG, PG and PC, with surface pre-treatments; B) - Surface polarity of MG, PG and PC, with surface pre-treatments

Surface polarities for each substrate pre-treatment condition were calculated and are presented in Figure 46. Surface polarity summary:

IPA treatment: Polycarbonate (6.7%) < Glass (13.4%) < Magnesium (26.3%)

Plasma treatment: Polycarbonate (31.3%) < Glass (37.2%) < Magnesium (41.7%)

Polycarbonate increased the surface polarity by a factor of 5, which was the highest increment using plasma pre-treatment. Despite having a low polar value, it almost reach MG and PG surface free energies. Plasma surface pre-treatment is more significant for PC, comparing to the other substrates.

The mean values of polar contact angle and dispersive contact angle for all samples are presented in Table 11 and in Figures 47.

Table 11 - Polar and dispersive contact angle measurements

# Test	Substrate	Treatment	θ^{H_2O} (°)	StandDev (°)	$\theta^{CH_2I_2}$ (°)	StandDev (°)
#1 - #5	MG	None	78.608	± 4.159	63.556	± 0.763
#6 - #10		IPA	70.542	± 1.676	59.552	± 0.343
#11 - #15		Plasma	42.040	± 1.975	48.514	± 2.155
#16 - #20	PG	None	85.426	± 1.410	31.046	± 5.140
#21 - #25		IPA	73.878	± 3.977	41.158	± 1.536
#26 - #30		Plasma	35.718	± 1.490	35.794	± 2.861
#31 - #35	PC	None	81.580	± 1.367	34.470	± 3.888
#36 - #40		IPA	78.674	± 3.585	30.314	± 0.739
#41 - #45		Plasma	46.094	± 1.932	34.712	± 0.793

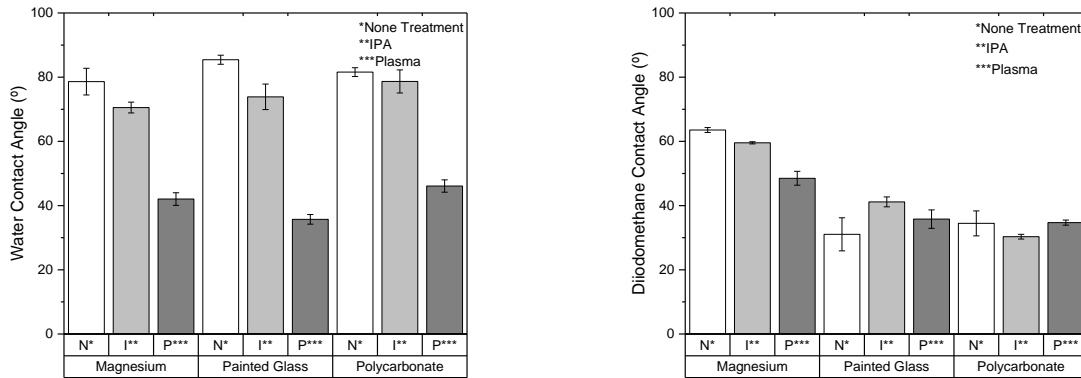


Figure 47 - Water contact angles and diiodomethane contact angles on MG, PG, PC substrates and IPA and plasma surface treatments

Water contact angle (polar) summary:

IPA treatment: Polycarbonate (78.7°) > Painted Glass (73.9°) > Magnesium (70.5°)
 Plasma treatment: Polycarbonate (46.1°) > Magnesium (42.0°) > Painted Glass (35.7°)

The contact angle of the polar component decreases with IPA cleaning and decreases even more with plasma treatment. Plasma pre-treatment influenced significantly polar contact angle but not dispersive contact angles. Plasma bombardment breaks hydrogen bonds from the polymeric chain or can split chains, producing free radicals, which are combined with oxygen from the air, increasing polarity [31].

Concluding, all substrates became more hydrophilic through both surface pre-treatments. However, Visteon SFE benchmark (50 mN/m) was only reached through plasma pre-treatment.

On the other hand, having the same surface energy does not mean having the same polar effect, for example the virgin and IPA cleaned painted glasses had 85.4° and 73.9° (polar contact angle) respectively, even though they have the same surface free energy (45mN/m).

Moreover, looking at contact angles of the PC sample, the dispersive component barely has any variation, while the polar contact angle is the one that revealed the true effectiveness of the plasma pre-treatment.

These two examples, make it clear that the effectiveness of pre-treatment surface could more simply characterized through only the polar component. Instead of the full characterization with the two liquids.

For economic reasons, it is proposed that Visteon can use only the water contact angle as the surface wettability characterization.

4.2 Adhesive Characterization

In this section, 3 glues, silane terminated polyurethane (MS1), silane terminated polyether (MS2) and silicone (SIL) and 1 acrylic double side tape with foam core (DST) were studied.

4.2.1 Hardness Test

The shore A hardness values were summarized in Table 12.

Table 12 - Shore A hardness results for MS1, MS2 and SIL adhesives

Time (h)	MS1		MS2		SIL	
	Shore A Hardness	StandDev	Shore A Hardness	StandDev	Shore A Hardness	StandDev
0,5	-	-	38.000	±0.100	-	-
1	7.860	±0.167	42.040	±0.055	-	-
2	18.120	±0.084	45.620	±0.130	-	-
4	29.200	±0.122	46.680	±0.130	23.020	±0.130
8	38.840	±0.089	48.360	±0.114	26.680	±0.249
12	41.720	±0.084	49.100	±0.100	27.220	±0.164
24	46.500	±0.187	49.520	±0.130	27.360	±0.152

MS1 and SIL, at 30 minutes after dispensing, were not stiff enough for the hardness measurements. On the other hand, only MS2 hardness was measurable at such short period of time. This was a key indication that the MS2 cure is faster than the MS1 counterpart and the SIL (Figure 48). Curing percentage was presented in Table 13, considering the full cured hardness values from the manufacturer's datasheets (Equation 10).

$$Cure (\%) = \frac{Experimental\ Hardness}{Full\ Cured\ Hardness\ (Datasheet)} \quad (10)$$

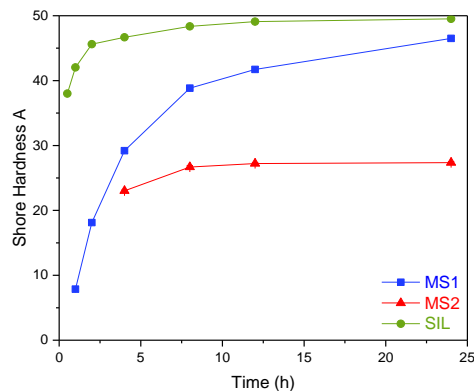


Figure 48 - Shore A hardness vs. time for MS1, MS2 and SIL adhesives

Table 13 - Adhesives curing rate over time (h)

Time (h)	MS1	MS2	SIL
	Cure (%)	Cure (%)	Cure (%)
0.5	-	69.09	-
1	15.41	76.44	-
2	35.53	82.95	-
4	57.25	84.87	76.73
8	76.16	87.93	88.93
12	81.80	89.27	90.73
24	91.18	90.04	91.20

The main goal of these tests was to understand the curing state of the glue as a function of curing time, particularly between 30 and 120 minutes using a simple metric. 30 minutes after dispensing, only MS2 was able to be measured, and which was already 69.09% full cured hardness. MS1 and MS2, 1 hour after dispensing were 15.41% and 76.44% respectively, of maximum hardness. In 2 hours MS1 was 35.53% and MS2 was 82.95% of their maximum hardness. No measurement was obtained for SIL for the two-hour interval after dispensing, because was not cured enough. Summarizing, it was expected that MS2 cures faster and obtained higher compression strength than SIL and MS1, between 2 hours, after dispensing.

Even using measurement processes according to the standard, results were always operator dependent, and this was the biggest source of variability in the results, particularly for lower hardness values.

4.2.2 Compression Test

All materials had the same pattern behavior. An average displacement was calculated as a function of the applied load.

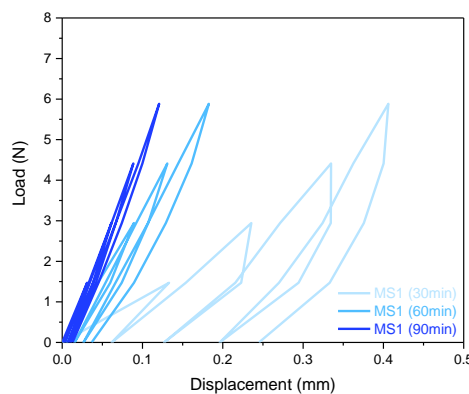


Figure 49 - Load (N) vs. displacement (mm) graph for adhesive MS1, cured for different times: 30, 60 and 90 minutes

In Figure 49, the area under the loading curve can be called the input energy. During the unloading, not all the initial energy was recovered. The energy that was not returned was converted into heat by hysteresis. In the case of viscoelastic materials, hysteresis is due to the viscous component of their properties. If the material were purely elastic, there would be less resistance to the force applied, resulting in less energy being applied [44].

The load (N) was converted to compression stress (σ), (Equation 11), and displacement (ϵ) to strain (%) (Equation 12). Stress (MPa) vs strain (%) was plotted in Figures 50, 51, 52 and 53.

$$\sigma = \frac{F}{A} \tag{11}$$

$$\epsilon = \frac{\Delta L}{L_0} \tag{12}$$

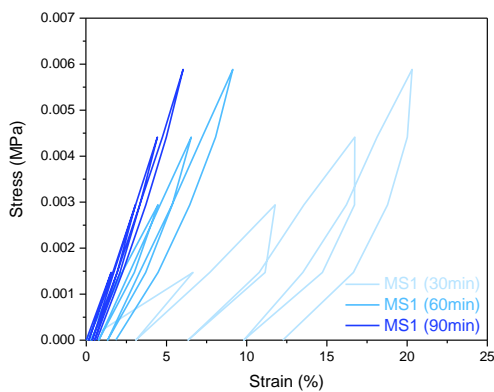


Figure 50 - Stress (MPa) vs. Strain (%) graph for MS1 adhesive, cured for different times: 30, 60 and 90 minutes

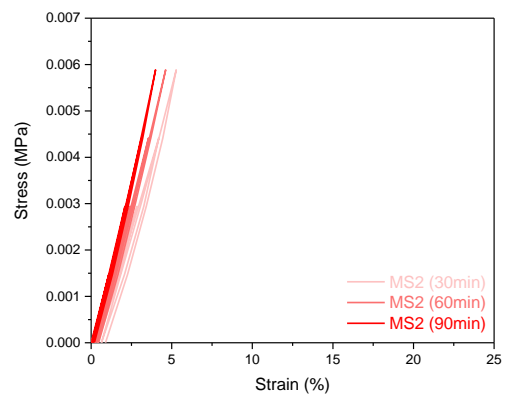


Figure 51 - Stress (MPa) vs. Strain (%) graph for MS2 adhesive, cured for different times: 30, 60 and 90 minutes

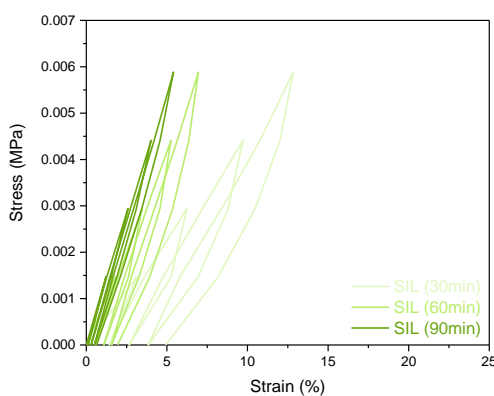


Figure 52 - Stress (MPa) vs. Strain (%) graph for SIL adhesive, cured for different times: 30, 60 and 90 minutes

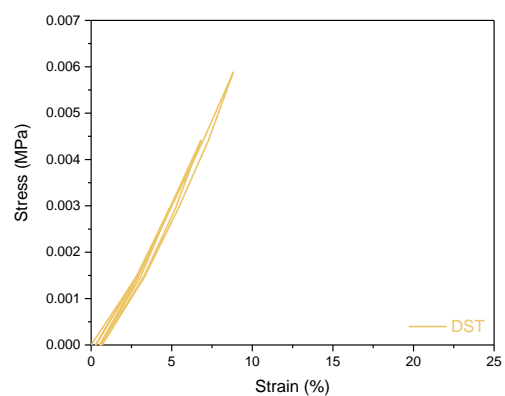


Figure 53 - Stress (MPa) vs. Strain (%) graph for DST

All adhesives exhibit the same pattern of behavior as a function of curing time, a nonlinear plastic behavior. Plastic strain is initiated at the yield point and involves energy dissipation, resulting in irreversible deformation. In this study that all structural adhesive strains were beyond the yield point. When unloaded the adhesive bead did not recovery to the original height.

The compressive strength (MPa) vs. maximum strain (%) was plotted, for each curing time, for all adhesives (Figures 54, 55, 56 and 57).

Adhesives exhibit both viscous and elastic behaviors as they are viscoelastic materials. Figure 66 showed that the adhesives were more cured, as more time had passed since the dispensing, i.e. the longer the curing time. The slope can be looked as the elastic modulus showing that the higher the slope, the higher the curing rate, the higher the adhesive stiffness. Something with a higher slope will deform less than an adhesive with a lower slope. Linear regression for all plots are presented in Table 14 and in Figure 58.

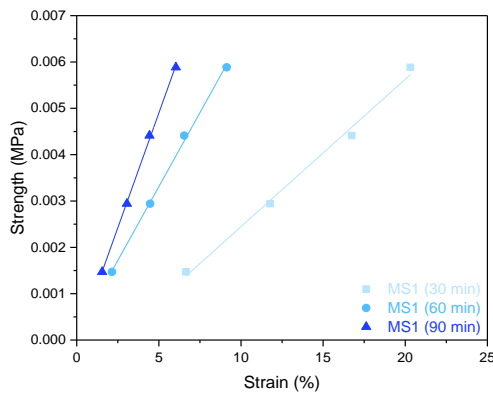


Figure 54 - Compression strength (MPa) vs. strain (%) of MS1 (30, 60 and 90 minutes cure)

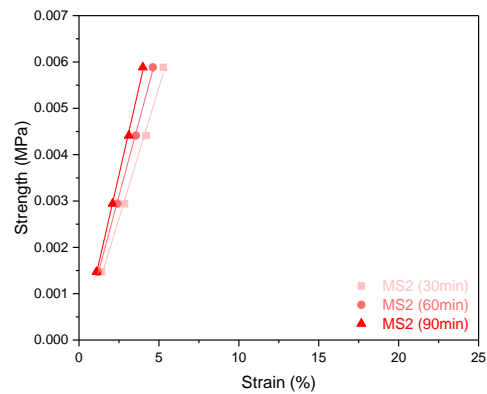


Figure 55 - Compression strength (MPa) vs. strain (%) of MS2 (30, 60 and 90 minutes cure)

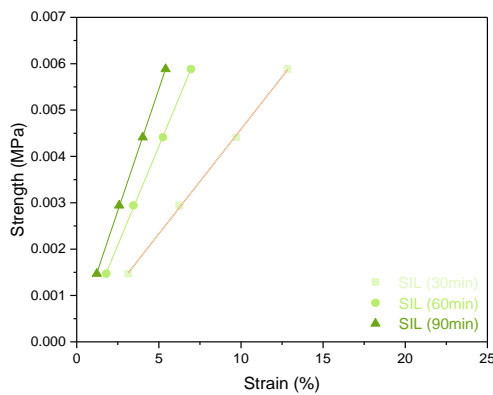


Figure 56 - Compression strength (MPa) vs. strain (%) of SIL (30, 60 and 90 minutes cure)

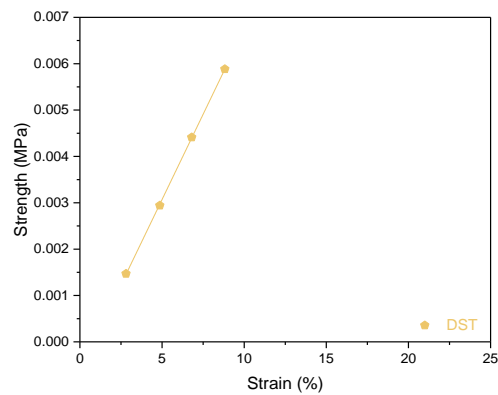


Figure 57 - Compression strength (MPa) vs. strain (%) of DST

Table 14 - Linear regression for all adhesives at different curing times (30, 60 and 90 minutes)

Adhesive	Curing Time (min)	Linear Regression	R ²
MS1	30	$y = 3.2 \times 10^{-4}x - 0.00074$	0.99361
	60	$y = 6.4 \times 10^{-4}x + 0.00012$	0.99826
	90	$y = 9.8 \times 10^{-4}x - 0.00006$	0.99914
MS2	30	$y = 1.13 \times 10^{-3}x - 0.00022$	0.99613
	60	$y = 1.28 \times 10^{-3}x - 0.00009$	0.99902
	90	$y = 1.51 \times 10^{-3}x - 0.00021$	0.99871
SIL	30	$y = 4.5 \times 10^{-4}x + 0.00007$	0.99949
	60	$y = 8.5 \times 10^{-4}x - 0.00005$	0.99979
	90	$y = 1.05 \times 10^{-3}x + 0.00020$	0.99999
DST	-	$y = 7.4 \times 10^{-4}x - 0.00060$	0.99999

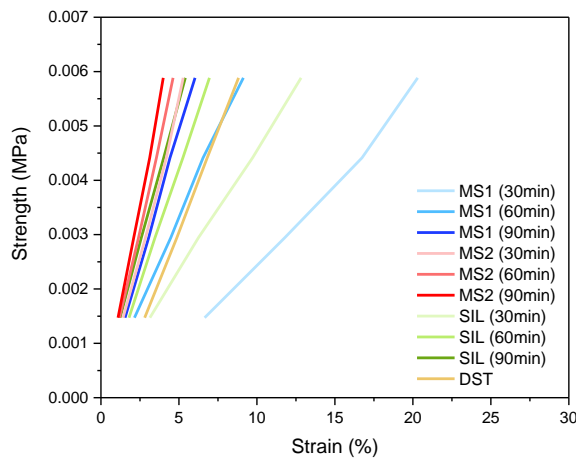


Figure 58 - Linear regression from strength vs. strain plots for all adhesives

The higher the lines clustering, the fastest the curing (Figure 58). There is a big curing rate difference between silane-modified polyurethane (MS2) and silane-modified polyether (MS1). MS2 cures fast than MS1, confirming the hardness curing rate results.

Linear regressions were comparable for a single curing time, as the applied loads were constant (Figure 58). MS2 obtained the highest slope for every curing time: 30 minutes ($y=1.13 \times 10^{-3}x$), 60 minutes ($y=1.28 \times 10^{-3}x$), and 90 ($y = 1.51 \times 10^{-3}x$).

Using DST as a benchmark, the table 15 shows how much time the glue need to reach the same stiffness.

Table 15 - Minimum curing time for MS1, MS2 and Sil to obtain DST slope benchmark

Adhesive	DST Benchmark	Adhesive Slope	Minimum Curing Time
MS1	$y = 7.4 \times 10^{-4}x$	$y = 9.8 \times 10^{-4}x$	90 minutes
MS2		$y = 1.13 \times 10^{-3}x$	30 minutes
SIL		$y = 8.5 \times 10^{-4}x$	60 minutes

Comparing the linear equations of acrylic double side tape and those of the other glues, it is concluded that silane-modified 2 requires shorter holding time, before the screwing process, than silicone and silane-modified 1 adhesives (Table 13).

This approach will be applied in real environment, and the results will be clearer, with a strain estimation for a real display case study, using the linear regression obtained in these compression test.

4.2.3 Lap Shear Test

Lap Shear tests were done to evaluate the mechanical strength of different single lap joints.

1st Methodology

The substrates were the only variable between the three series. Through the data collected it was possible obtain load vs. displacement plots. As an example, Figure 59 shows five (#11 - #15) load vs. displacement plots.

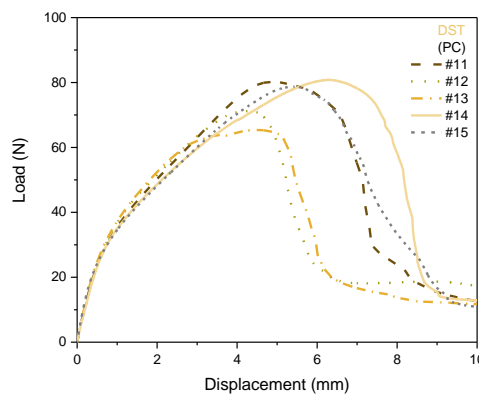


Figure 59 - Load vs. displacement plot for DST adhesive joints using IPA on PC as surface pre-treatment (#11 - #15)

Average maximum load was calculated for all tests. Table 16, 17 and 18 show the mean values of the maximum force for each series of specimens, and the standard deviation associated with each of the means.

Table 16 - Average maximum load using magnesium substrate

Magnesium		
#Test	Displacement (mm)	Maximum Load (N)
#1	2.370	48.155
#2	4.973	73.188
#3	4.757	62.900
#4	4.207	69.194
#5	3.397	65.612
Average		63.810
StanDev		± 8.557

Table 17 - Average maximum load using glass substrate

Glass		
#Test	Displacement (mm)	Maximum Load (N)
#6	4.503	66.250
#7	4.533	68.506
#8	3.727	57.201
#9	4.123	49.737
#10	5.263	75.546
Average		63.448
StanDev		± 9.020

Table 18 - Average maximum load using polycarbonate substrate

Polycarbonate		
#Test	Displacement (mm)	Maximum Load (N)
#11	4.817	80.164
#12	4.310	71.213
#13	4.463	65.401
#14	6.290	80.822
#15	5.435	78.800
Average		75.280
StanDev		± 6.018

Figure 60 shows all average maximum load values. Shear strength was obtained by dividing the average maximum load by the adhesive contact area (312.5mm²) (Equation 13) (Figure 61) [45].

$$\text{Shear Strength (MPa)} = \frac{\text{Maximum Applied Load (N)}}{\text{Adhesive Area (mm}^2\text{)}} \quad (13)$$

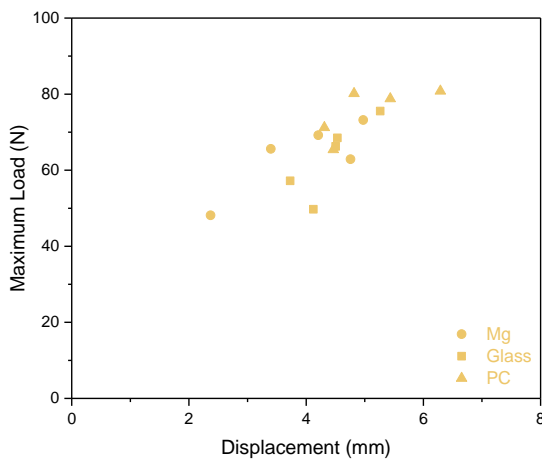


Figure 60 - Average maximum load (N) vs. displacement (#1 - #15)

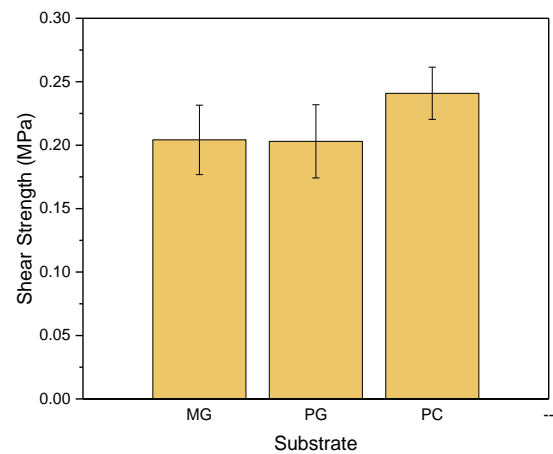


Figure 61 - DST shear strength for all 3 substrates (MG, PG and PC)

Failure modes of this methodology were summarized in Table 19. Analysing all samples, was verified that all the specimens failed adhesively, which means that the failure occurs between the adhesive and the adherent. It was expected because tests were done with double side tapes and tapes usually have more cohesive strength than adhesive strength.

Table 19 - 1st Methodology failure modes




Adhesive	Magnesium	Glass	Polycarbonate
DST	 Adhesive Failure	 Adhesive Failure	 Adhesive Failure

Table 20 -1st Methodology DST shear strength results and failure modes

# Sample	Adhesive	Substrate	Average Maximum Load (N)	Standard Deviation (N)	Lap Shear Strength (MPa)	Standard Deviation (MPa)	Failure Mode
#1 - #5	DST	MG	63.810	± 9.020	0.204	± 0.032	Adhesive
#6 - #10		PG	63.448	± 8.557	0.203	± 0.031	Adhesive
#11 - #15		PC	75.280	± 6.018	0.241	± 0.022	Adhesive

There was no significant shear strength difference between all adhesive joints (Table 20). Polycarbonate was considered the best substrate used because obtained the highest shear strength. A possible reason could be due to the pressure sensitive nature of the DST adhesive (pressure sensitive adhesive). During DST bonding a set of 500 g weight was used to apply pressure and could be possible that the pressure was not uniformly distributed, meaning the tape could not be fully wetting all surfaces.

Overall, it is observed that PC is an acceptable choice to use for the next methodology, as was originally planned.

2nd Methodology

The second methodology compares the adhesives shear behavior over time (30, 60 and 90 minutes), using isopropanol cleaning as the only surface pre-treatment and polycarbonate as the only substrate, as it was more easily obtained sample. Even though polycarbonate might not be the ideal substrate, the data collected allowed for comparison and concluding. Each series was tested on 5 samples.

All maximum loads were obtained from load vs displacement plots. For each series, the average maximum load and the standard deviation was calculated. These values as a function of curing time, are presented in Figure 62. The obtained maximum load values were converted into shear stress, to compare the behavior of the different adhesive joints. Shear strengths are obtained dividing the average maximum load by the adhesive contact area (Equation 13) (Figure

63). Table 21 showed the mean values of maximum force and shear strength for each series of specimens and the respective standard deviation for every series.

Table 21 - Shear Load (N) and shear strength (MPa) for all 4 adhesives using PC substrate and IPA as surface pre-treatment

# Sample	Adhesive	Substrate	Treatment	Curing Time (min)	Maximum Load (N)	Standard Deviation (N)	Lap Shear Strength (MPa)	Standard Deviation (MPa)
#11 - #15	DST	PC	IPA	-	75.280	± 6.018	0.241	± 0.022
#16 - #20	MS1			30	1.519	± 0.709	0.005	± 0.002
#21 - #25				60	65.137	± 5.596	0.208	± 0.018
#26 - #30				90	86.716	± 9.260	0.277	± 0.030
#31 - #35	MS2			30	196.340	± 9.942	0.620	± 0.032
#36 - #40				60	228.882	± 24.657	0.732	± 0.079
#41 - #45				90	298.501	± 15.444	0.955	± 0.049
#46 - #50	SIL			30	0.847	± 0.222	0.003	± 0.001
#51 - #55				60	2.432	± 0.258	0.008	± 0.001
#56 - #60				90	7.983	± 2.180	0.026	± 0.007

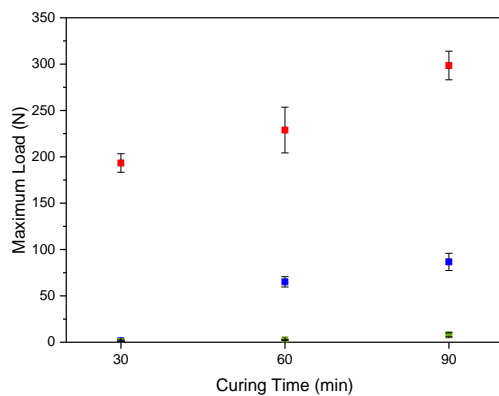


Figure 62 - Maximum load (N) vs. curing time (min) for MS1, MS2 and SIL

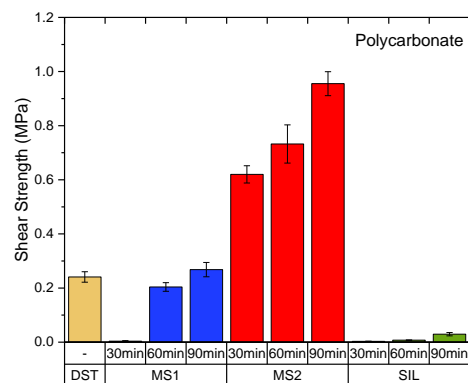


Figure 63 - Shear strength (MPa) for different curing times (DST, MS1, MS2 and SIL)

For all 3 different curing times, strength of:

Silicone < Silane-modified 1 < Silane-modified 2

Silicone had the lowest shear strength among all adhesives, and Silane-modified 2 was the adhesive that showed higher strength in all tests of the second methodology. These results were not expected before lap shear tests, as MS1 full cured shear strength (3MPa) is higher than MS2 (2MPa) and SIL (1MPa).

MS1 showed higher shear strength than SIL, but only with 90 minutes of curing time MS1 has higher shear strength than DST adhesive. At 30 minutes curing time, MS2 showed a higher

strength than acrylic double side tape. DST shear strength results are a good comparison reference, because it maintains its shear strength over time. Furthermore, it is an adhesive utilized in industry.



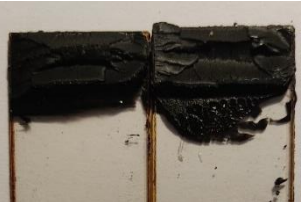






Table 22 showed an estimation of curing ratio for all glues at different curing times, based on the final curing strength from the manufacturer datasheets. In all 3 curing times silane-modified 2 showed higher full cured strength ratio.

Although less cured compared to the hardness tests, MS2 also cured fastest, followed by MS1 and SIL. Comparing curing rate by both tests (shore A hardness and lap shear), MS2 were 69.9% and 31%, respectively at 30 minutes curing time. At 60 minutes curing time, MS2 was 76.4% cured by shore A hardness, but lap shear tests results indicated that MS2 was only 36.6% cured.

Table 22 - Curing time estimation for three glues (MS1, MS2 and SIL)

Time (min)	MS1	MS2	SIL
	Cure (%)	Cure (%)	Cure (%)
30	0.17	31.00	0.30
60	6.93	36.60	0.80
90	9.23	47.75	2.60

Table 23 - 2nd Methodology failure modes

Adhesive	30 minutes	60 minutes	90 minutes
MS1	 Cohesive Failure	 Cohesive Failure	 Cohesive Failure
MS2	 Mixed Failure	 Mixed Failure	 Mixed Failure
SIL	 Adhesive Failure	 Adhesive Failure	 Adhesive Failure

Although the same basic chemistry, the mechanical shear behavior is completely different. MS2 quickly reached high strength but then grew slowly. MS1 grew slowly but final strength is higher than MS2. Silicone results were not expected. SIL build-up was too low and showed low adhesion. These results may have been due to the substrate used (PC), due to the curing activation, or due to the 2 mm bead thickness. The thicker the bead, the lower the final shear strength. Besides shear strength values, failure mode analysis was also an objective. Photographs were taken of the specimens after the respective tests to analyse their failure modes. The joint failures were shown in Table 23.

As DST, all silicone samples (#46 - #60), using polycarbonate as adherent, presented adhesive failure. Even after 90 minutes, SIL glue looks pasty, not showing enough strength to resist to the shear forces applied. All silane-modified 2 series (#31 - #45), showed mixed failure. Silane-modified 1 samples (#16-#30) presented cohesive failure, which is preferable than adhesive failure. A cohesive failure mode, mean that the bond strength is stronger than the forces holding the bulk of the adhesive together.

3rd Methodology

The third methodology goal was to test the surface treatment effect on the shear strength of the adhesive joints. Isopropanol and plasma were the chosen surface pre-treatments in this thesis. In this method, the only constant was the type of adhesive (MS2), because of the better performance shown in the previous methodology. Lap shear samples were done using all three substrates and were tested 10 minutes and 30 minutes after dispensing (Figures 64, 65 and 66).

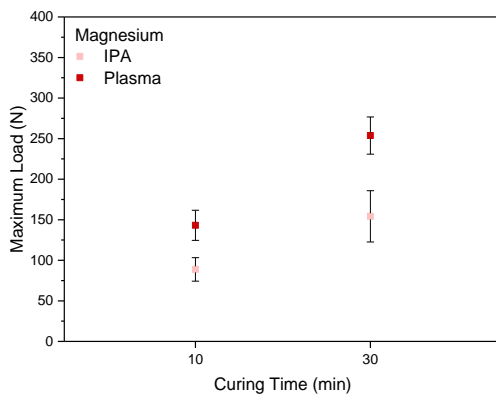


Figure 64 - MS2 maximum load (N) using IPA and plasma pre-treatments on magnesium substrate

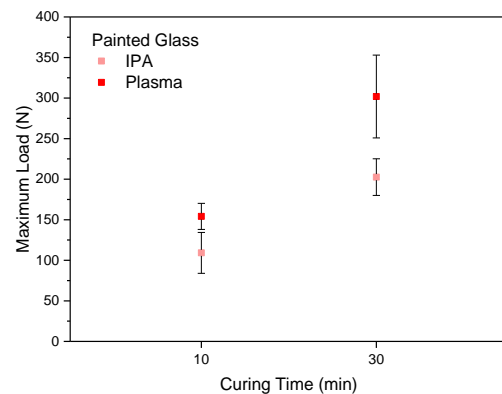


Figure 65 - MS2 maximum load (N) using IPA and plasma pre-treatments on painted glass substrates

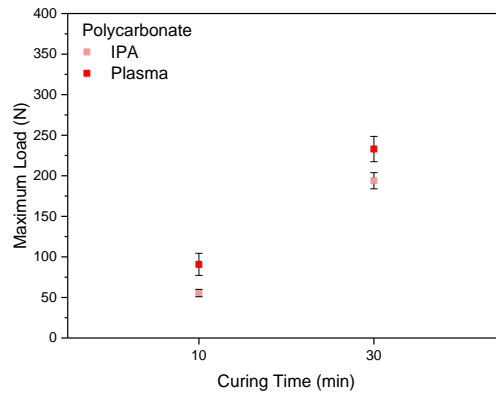


Figure 66 - MS2 maximum load (N) using IPA and plasma pre-treatments on polycarbonate substrate

Table 24 was obtained after averaging and converting the maximum load, obtained from lap shear data, to shear strength.

Table 24 - Shear load (N) and shear strength (MPa) over time for MS2 using MG, PG and PC substrates and IPA and plasma surface pre-treatments

# Test	Adhesive	Substrate	Curing Time (min)	Treatment	Average Maximum Load (N)	Standard Deviation (N)	Average Shear Strength (MPa)	Standard Deviation (MPa)
#61 - #65	MS2	Magnesium	10	IPA	88.768	± 14.513	0.284	± 0.046
#66 - #70				Plasma	143.156	± 18.601	0.458	± 0.060
#71 - #75			30	IPA	154.192	± 31.639	0.493	± 0.101
#76 - #80				Plasma	253.784	± 22.884	0.812	± 0.073
#81 - #85		Painted Glass	10	IPA	109.164	± 25.189	0.349	± 0.081
#86 - #90				Plasma	154.116	± 16.071	0.493	± 0.051
#91 - #95			30	IPA	202.523	± 22.603	0.648	± 0.072
#96 - #100				Plasma	301.915	± 51.095	0.966	± 0.164
#101 - #105		Polycarbonate	10	IPA	55.389	± 4.555	0.177	± 0.015
#106 - #110				Plasma	90.820	± 13.605	0.291	± 0.044
#31 - #35			30	IPA	196.340	± 9.942	0.620	± 0.032
#111 - #115				Plasma	232.937	± 15.637	0.745	± 0.050

Figure 67 showed that the adhesive joint strength increased with longer curing times and with plasma surface treatment. Painted glass was the adherent that showed the highest strength in all conditions.

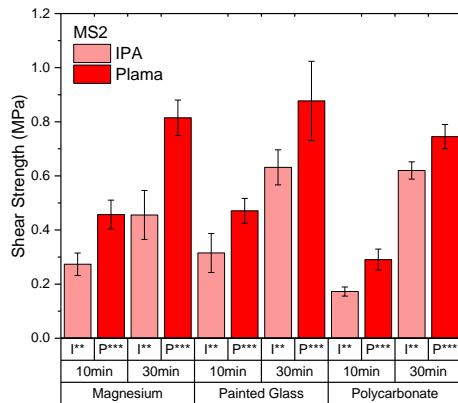


Figure 67 - MS2 shear strength adhesive results over time (10 and 30 minutes) using IPA and plasma pre-treatments on polycarbonate substrate

At 10 minutes:

IPA, Polycarbonate (0.177 MPa) < Magnesium (0.284 MPa) < Painted Glass (0.349 MPa)
 Plasma, Polycarbonate (0.291 MPa) < Magnesium (0.458 MPa) < Painted Glass (0.493 MPa)

At 30 minutes

IPA, Magnesium (0.493 MPa) < Polycarbonate (0.620 MPa) < Painted Glass (0.648 MPa)
 Plasma, Polycarbonate (0.745 MPa) < Magnesium (0.812 MPa) < Painted Glass (0.966 MPa)





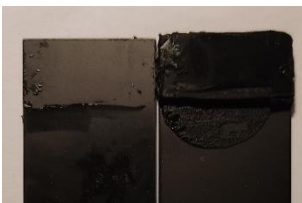






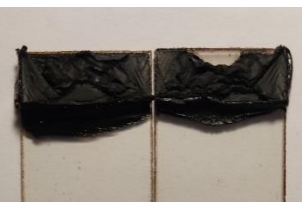
Using the same substrate and a single surface pre-treatment, the results of the 1st methodology (DST) were more similar to each other than those of the 3rd methodology (MS2). Even the substrates that showed the best behavior were different. MS2 behaved better with painted glass and DST behaved better with polycarbonate. These results suggested that adhesives have different behaviors for different substrates.

Results from 3rd Methodology using plasma treatment were all expected. According to previous contact angle results, using plasma treatment: Polycarbonate (46.1°) > Magnesium (42.0°) > Painted Glass (35.7°), lower contact angle, better wettability, higher shear strength.

The higher increase in strength, as a function of curing time, occurred using plasma and glass as the substrate, which increased 0.473 MPa. The largest percent increase in strength 266.7 %, occurred using isopropanol and polycarbonate as the substrate. The higher increase in strength, as a function of surface treatment, in value and percentage, were using magnesium as an adherent, and occurred at 30 minutes of curing. It increased by 0.319 MPa, which is equivalent to 64.7 %.

In Figure 67, it was cleared that plasma pre-treatment increased initial shear strength, which means that it is relevant in initial behavior, as well as in final full cure behavior. Table 25 showed failure mode for each series of the third methodology.

Table 25 - 3rd Methodology failure modes

Subst.	10 minutes		30 minutes	
	IPA	Plasma	IPA	Plasma
MG	 Cohesive/ Mixed Failure	 Cohesive Failure	 Adhesive Failure	 Mixed Failure
PG	 Adhesive Failure	 Cohesive Failure	 Adhesive Failure	 Cohesive Failure
PC	 Cohesive Failure	 Cohesive Failure	 Mixed Failure	 Mixed Failure

In all 10 minutes series, it was observed that all adhesives were still in a paste like appearance. This caused cohesive failure in many of the cases. In cohesive failures the bonding of the adhesive to the substrate is stronger than the internal strength of the adhesive itself.

After 30 minutes of curing time, the adhesive was already stiffer and there were no cohesive failures without plasma application. After 30 minutes the failures on glass and magnesium were adhesive and on polycarbonate were adhesive and cohesive. The plasma, after 30 minutes was very effective, going from adhesive failure to mixture and to cohesive failure, on magnesium and the glass respectively.

Concluding, silane-modified 2 was the adhesive that showed the fastest curing time as well as the highest strength during the first 90 minutes of curing. Plasma pre-treatment significantly improved the adhesion of the joints, which achieved higher strengths whenever plasma was used. The use of plasma pre-treatment in production should be mandatory.

4.3 Assembly Forces

In this chapter, the acceleration forces and the forces resulting from the screwing process have been characterized using real assembly processes (Figures 68 and 69). This display had 4000mm² adhesive area and weighs 790g (carrier + lens).



Figure 68 - Visteon display lens



Figure 69 - Visteon display carrier

4.3.1 Screwing Forces

The obtained mass data were converted into load values. The sum of the five cells load were plotted for the three samples (Figures 70, 71 and 72).

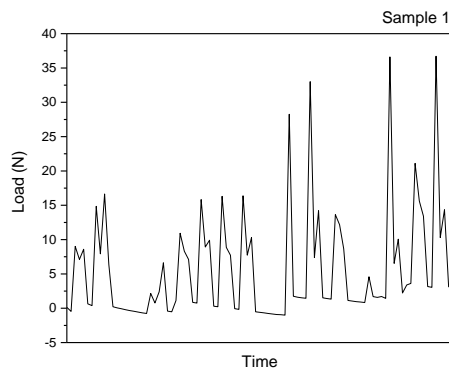


Figure 70 - Sample 1 screwing load (N) over time

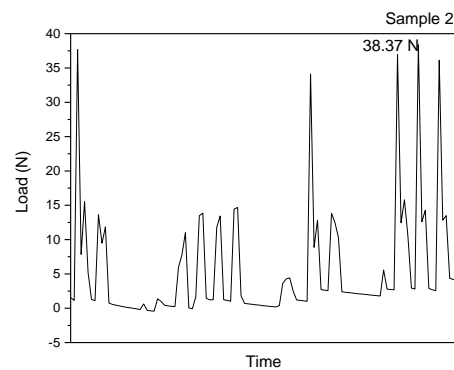


Figure 71 - Sample 2 screwing load (N) over time

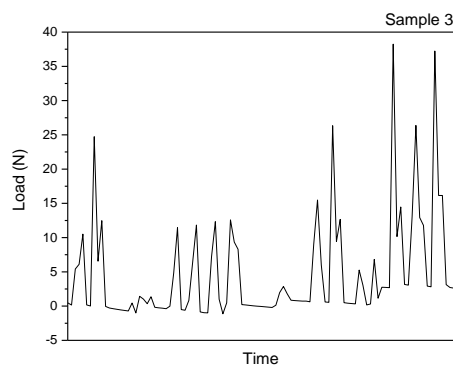


Figure 72 - Sample 3 screwing load (N) over time

The maximum force applied by the screwing process was 38.37 N, which occurred on the second sample. 36.72 N and 38.24 N were the highest force applied for the first and the third sample, respectively.

Visteon Display

Screwing forces result in compression forces on the display adhesive joints. The holding times needed before screwing were estimated using compression tests results. This estimation was made using a real Visteon display (Figure 73). Display had 4000 mm² of adhesive area.



Figure 73 - 2D Visteon display carrier

Dividing the screwing process maximum force, 38.37 N, by the products adhesive area 4000 mm², a compression strength of 0.153 MPa, was obtained resultant of the screwing process. The strain for each adhesive with different curing time, was obtained using the 0.153 MPa strength in the linear equations obtained in the compression tests (Table 26).

Visteon defines 15% as maximum strain specification.

Table 26 - Ok / Not ok

Adhesive	Curing Time (min)	Linear Regression	Strain (%)	OK/NOK
MS1	30	$y = 3.2 \times 10^{-4}x - 0.00074$	32.29	NOK
	60	$y = 6.4 \times 10^{-4}x + 0.00012$	14.80	OK
	90	$y = 9.8 \times 10^{-4}x - 0.00006$	9.85	OK
MS2	30	$y = 1.13 \times 10^{-3}x - 0.00022$	8.68	OK
	60	$y = 1.28 \times 10^{-3}x - 0.00009$	7.56	OK
	90	$y = 1.51 \times 10^{-3}x - 0.00021$	6.49	OK
SIL	30	$y = 4.5 \times 10^{-4}x + 0.00007$	21.16	NOK
	60	$y = 8.5 \times 10^{-4}x - 0.00005$	11.34	OK
	90	$y = 1.05 \times 10^{-3}x + 0.00020$	8.95	OK
DST	-	$y = 7.4 \times 10^{-4}x - 0.00060$	13.77	OK

With the simulation it is reinforced that the be benchmark on the previous chapter for the compression test, using DST as a reference, is adequate as the DST strain (13,77 %) is within Visteon maximum strain specification (15 %).

Both, MS1 and SIL, with 30 minutes of curing time, showed a strain higher than 15% and therefore not acceptable for this thesis process. But MS1 and SIL with 60 minutes and 90 minutes of curing time, exhibited better performance than the DST benchmark. The same linear equations were used to determine the minimum area for a maximum strain of 15 % during the screwing process for MS1 and SIL adhesives (Table 27).

A Visteon display example was used for a better interpretation of the results. MS2 was the adhesive that showed the lowest strain, 6.49 % at 90 minutes after bonding. MS2 strain at 30 minutes is lower than that for DST, and lower than MS1 and SIL, with 90 minutes of holding time. These results were already expected from the linear equations from previous chapter. Once again, MS2 showed better mechanical performance.

MS1 and SIL exhibited a minimum area of 9451 mm² and 5626 m², respectively, if a screwing operation is desired before 30 minutes, after bonding.

Table 27 - Minimum area to assure Visteon strain specification (15%)

Adhesive	Curing Time (min)	Linear Equation	Strain (%)	Stress (Mpa)	Minimum Area (mm ²)
MS1	30	$y = 3.2 \times 10^{-4} x - 0.00074$	15	0.00406	9451
SIL	30	$y = 4.5 \times 10^{-4} x + 0.00007$	15	0.00682	5626

Only MS1 and SIL presented more than 15 % strain after 30 minutes of curing for this Visteon display example. But if the adhesive area of MS1 and SIL increases from 4000 mm² to 9451 mm² and 5626 m², respectively, only 30 minutes of holding time are required before the screwing process (Table 28) and, therefore, could be also potential adhesive solution for this application. These means that product design is also relevant and not only material properties.

Table 28 - Minimum holding time before screwing process for all glues

Adhesives	Screwing Process
MS1	60 min
MS2	10 min
SIL	60 min

4.3.2 Acceleration Forces

After processing all data of the nine tests, acceleration results were plotted for each direction (X, Y and Z). Figures 74, 75 and 76 were illustrative of the plots obtained.

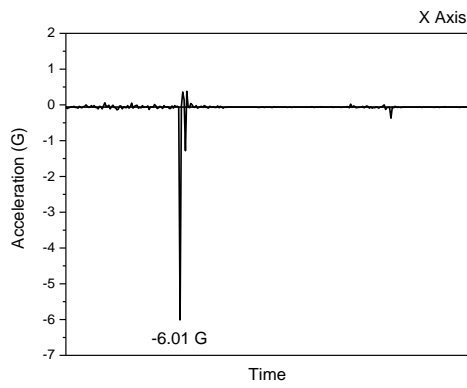


Figure 74 - Acceleration on X direction (#7 test)

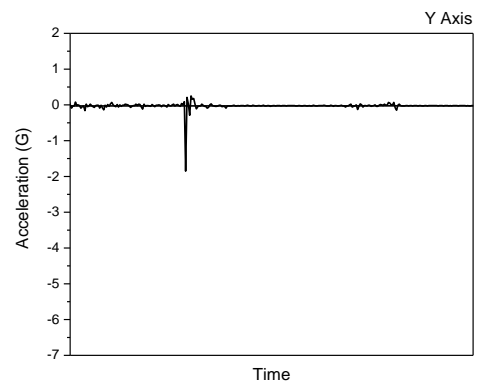


Figure 75 - Acceleration on Y direction (#7 test)

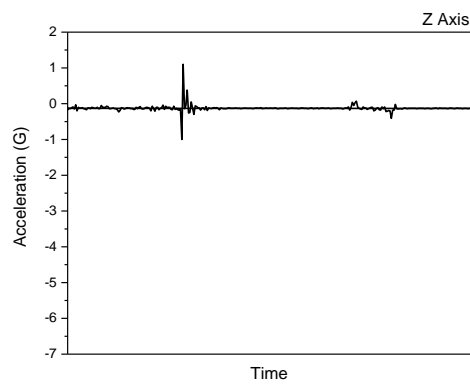


Figure 76 - Acceleration on Z direction (#7 test)

For each test, the highest value of the acceleration in all three axes was selected, Table 29.

Table 29 - Maximum acceleration (m/s²) at different velocities (120 mm/s, 175 mm/s, 230 mm/s)

# Test	Pallet Velocity (mm/s)	X Acceleration (G)	Y Acceleration (G)	Y Acceleration (G)	Maximum Acceleration (G)	Maximum Acceleration (m/s ²)
#1	120	1.84	0.50	0.71	1.84	18.04
#2		2.15	0.48	0.96	2.15	21.08
#3		0.87	0.71	0.93	0.93	9.12
#4	175	1.69	0.50	0.81	1.69	16.57
#5		2.71	0.45	0.68	2.71	26.58
#6		2.79	0.55	1.09	2.79	27.36
#7	230	6.01	1.85	2.08	6.01	58.94
#8		5.19	1.89	3.38	5.19	50.90
#9		5.05	0.86	1.23	5.05	49.52

The maximum acceleration of 6.01 G was obtained in the direction of pallet motion (x direction), with a pallet velocity of 230 mm/s. Converting, 58.94 m/s² was the maximum acceleration obtained by the movement of the pallet along the cell.

Visteon Display

Acceleration forces results in shear forces on the display adhesive joints. In this section all data obtained from the shear tests were used to estimate the holding time required before pallet movement for all four adhesives. This estimation was made with a real display, produced by Visteon (Figure 77). Visteon display has 790 g and 4000 mm² of adhesive area.



Figure 77 - 2D Visteon display lens

Maximum acceleration force could be obtained, applying Newton's second law (Equation 14), as it is known the mass of a real product. Dividing this maximum force by the products adhesive area, one can obtain the maximum stress by resulting from the movement of the pallets (Equation 15).

$$F = m \cdot a = [Kg] \cdot \left[\frac{m}{s^2}\right] \quad (14)$$

$$\tau = \frac{F}{A} = \frac{[N]}{[m^2]} \quad (15)$$

Acceleration forces and acceleration strengths were calculated using Equation 14 and Equation 15, respectively. All results were presented in Table 30.

Table 30 - Acceleration strength for different pallet velocities

	Pallet Velocity (mm/s)	Maximum Acceleration (mm/s ²)	Acceleration Force (N)	Acceleration Strength (MPa)
Acceleration Forces	120	21.084	16.657	0.067
	175	27.361	21.615	0.086
	230	58.938	46.561	0.186

Shear strength of the four adhesives were compared with the acceleration strength estimated for the display product. The minimum holding time before Visteon display starts moving after the bonding process, was therefore estimated, as shown in Table 31.

Table 31 - Minimum holding time before pallet movement for all adhesives

Adhesive	120 mm/s	175mm/s	230mm/s
DST	< 30 min	< 30 min	< 30 min
MS1	30min - 60min	30min - 60min	30min - 60min
MS2	< 10 min	< 10 min	10min - 30 min
SIL	> 90 min	> 90 min	> 90 min

MS1 and SIL needed to hold more than 30 minutes before moving after the bonding process. On the acceleration process characterization, it was clear that, the lower the velocity of the pallet movement, the lower the forces applied on the product. This suggested that the pallet velocity reduction results in reduction of the holding time after bonding. To reduce this holding time, it was made an estimation, by plotting acceleration strength vs. pallet velocity (Figure 78). By the linear equation $y = 0.00109x - 0.07719$, it was calculated the maximum velocity of the pallet, to reduce the holding time for 30 minutes, Table 32.

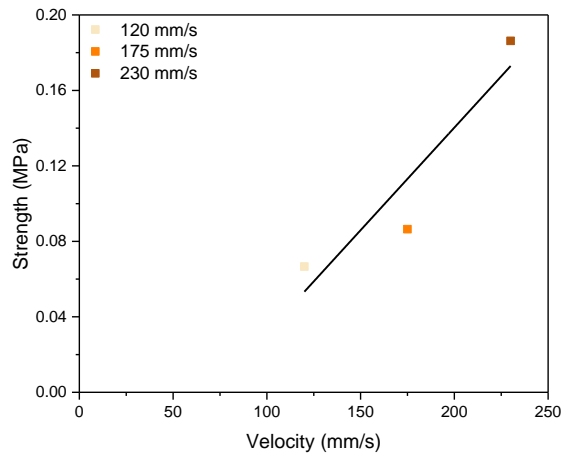


Figure 78 - Linear regression of strength (MPa) vs. velocity (mm/s), to reduce the holding time to 30 minutes

If the pallet moves at 75.4 mm/s, the MS1 holding time reduces to 30 minutes. SIL time reduces to 30 minutes with a pallet movement of 73.6 mm/s.

Table 32 - Maximum pallet speed (mm/s) to reduce the holding time to 30 minutes

Adhesive	Curing Time (min)	Shear Strength (MPa)	Speed (mm/s)
MS1	30	0.005	75.404
SIL	30	0.003	73.569

In all graphs, it is quite clear the pallet impact on the stopper, the descent and ascent movements of the conveyors, and the restart movement of the pallet (Figure 90).

The highest accelerations occurred in the X axis, 7 out of 8. All accelerations in Y were negligible. As expected, the accelerations in the X axis occurred at the beginning of pallet movement but specially on the impact of the pallet with the stopper. In the Z axis, accelerations only occurred with the movement of the conveyors.

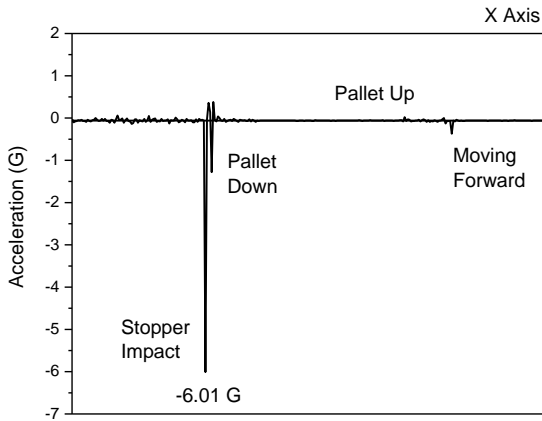


Figure 79 - Acceleration data (X axis)

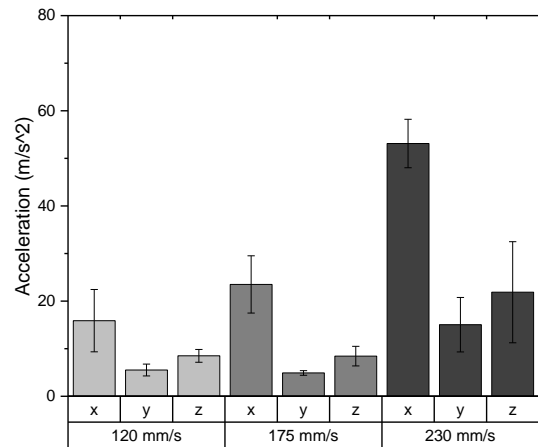


Figure 80 - Acceleration results at different speed (120 mm/s, 175 mm/s and 230 mm/s)

Only DST and MS2, used as structural adhesives on Visteon display exhibited a holding time lower than 30 minutes. MS2 requires only 10 minutes of holding time if the pallet moves at 175 mm/s on the other hand, MS1 and SIL require more than 30 minutes of holding time. However, if the pallet movement reduced to 75.4 mm/s and 73.6 mm/s, respectively, the holding time will be reduced to 30 minutes. It should be stressed that pallet's velocity can be reduced just a few instants before stopper impact to avoid a significantly extension of the assembly time.

6. Conclusion

The main purpose of this research was to study the curing state and the mechanical behavior of four adhesives for the selection of the best performing adhesive during the assembly process of an automotive display, short time frame compared with a full cured strength. For this reason, different adhesive joints (changing the adhesive, substrates, and surface-pre-treatment) and the main assembly forces processes were characterized.

Surface pre-treatment had a significant influence on the behavior of the adhesive joints. The surface treatment to be selected should increase the wettability of the substrate, and therefore, improve the adhesion of the adhesive, which causes an increase of the adhesive strength. Plasma pre-treatment was the one to promote, when compared to isopropanol cleaning. The highest increase on SFE was found to be on magnesium substrate: 16.2 % and 51.8 % for isopropanol and plasma, respectively. There were cases where the increase in SFE did not correspond to a decrease in water contact angle. Plasma is mainly responsible for the increase of the polar component (observed in all substrates), as such it is proposed to simplify surface characterization using only water contact angle.

Shore A Hardness measurements, were employed to estimate the state of cure of the studied structural adhesives as a function of time after dispensing. Silane-modified 2 achieved higher hardness values and faster curing than the other two adhesives, having achieved 69.09 % of the final hardness (reported by the suppliers) after 30 minutes of curing process.

Adhesives were mechanically characterized in order to compare their compression strength and shear strength to the stresses applied by the movement of the pallet and stresses resulting from the screwing process in the final assembly. In the compression tests, all adhesives exhibited the same nonlinear elastic behavior. The overlap of the compression stress-strain curves, in figure 52, also showed that silane-modified 2 cured faster than silane-modified 1 and silicone adhesives. Different curing times showed different linear equations for the compression strength vs. strain plots. The higher the slope, faster the adhesive curing. It was only possible to apply the obtained results quantitatively after the forces involved in the screwing process were characterized and using a real display adhesive contact area.

This research also analysed the mechanical shear behavior of different adhesive joints using 3 different methodologies. In the first methodology, substrates were the only existent variable. All samples used acrylic double side tape. Polycarbonate had a higher shear strength (0.24 ± 0.02 MPa) and the same adhesive failure as magnesium and painted glass. The second methodological objective was to test all adhesives using polycarbonate as a single substrate. The MS2 adhesive showed higher shear strength at the 3 different curing times. At 30 minutes curing time, Silane-modified 2 showed a higher strength (0.62 ± 0.03 MPa). In the third methodology, the greatest increase in strength occurred at 30 minutes of curing using the plasma pre-treatment

on magnesium substrate. It increased by 0.319 MPa, equivalent to 64.7 %. Surface pre-treatment also had an influence on the failure mode, improving from adhesive failures to mixed and cohesive failures.

Following the objectives, after a characterization of the substrates and adhesives, this research focused on characterizing 2 assembly forces: screwing forces and acceleration forces. 38.37 N was the maximum force applied in the screwing process. From acceleration forces characterization resulted that 58.94 m/s² was the maximum acceleration which occurs by moving the pallet along the cell, when a sudden stop occurs at a pallet speed of 230mm/s.

All research data was applied on a Visteon display example. Knowing the display mass and adhesive contact area data, it was estimated that after glue application, the silane-modified 2 requires less than 10 minutes of holding time, before being exposed to a pallet movement of 175 mm/s. The screwing process in the final assembly, could be done 30 minutes after dispensing and joining.

MS2 was selected as the best adhesive, due to its faster adhesion build-up compared to MS1 and SIL glues.

6.1 Future Studies

From this research several investigations can be developed:

- Verification of these research results within Visteon's production assemblies;
- FTIR analysis and DMA assays at different curing times, to deepen the knowledge of the curing state of MS2;
- Study of the ideal heights and speeds for plasma pre-treatment application;
- Study the mechanical behavior of adhesive joints through peel testing;
- Development of a method to characterize other forces applied on final assembly process e.g. clipping;
- Study the topography and roughness of the substrates after plasma pre-treatment.

7. References

- [1] Budzik, M. K. et al., Testing mechanical performance of adhesively bonded composite joints in engineering applications: an overview, *The Journal of Adhesion*, **2022**, 98, 2133-2209. [dx.doi.org/10.1080/00218464.2021.1953479](https://doi.org/10.1080/00218464.2021.1953479)
- [2] Feica, European Adhesives and Sealants Market 2021-2026, **2021** [Online]. Available: <https://www.feica.eu/information-center/market-reports>. [Accessed: 23-Jul-2022]
- [3] Jojibabu, P.; Zhanga, Y. X.; Prusty, B. G., A review of research advances in epoxy-based nanocomposites as adhesive materials, *International Journal of Adhesion and Adhesives*, **2020**, 96. [dx.doi.org/10.1016/j.ijadhadh.2019.102454](https://doi.org/10.1016/j.ijadhadh.2019.102454)
- [4] Maggiore, S. et al., A Review of Structural Adhesive Joints in Hybrid Joining Processes, *Polymers*, **2021**, 13. [dx.doi.org/10.3390/polym13223961](https://doi.org/10.3390/polym13223961)
- [5] Visteon, Products, [Online]. Available: <https://www.visteon.com/products/>. [Accessed: 16-Sep-2022]
- [6] Petrie E. M., Handbook of adhesives and sealants, 2nd ed. *The McGraw-Hill Companies, Inc.*, 2007
- [7] Santos C., Caracterização de Adesivos baseados em Dispersões Aquosas Vinílicas, Master Thesis, *Instituto Superior Técnico*, Universidade de Lisboa, 2008
- [8] Vashchuk, A. et al., Application of ionic liquids in thermosetting polymers: Epoxy and cyanate ester resins, *Express Polymer Letters*, **2018**, 12, 898-917. [dx.doi.org/10.3144/expresspolymlett.2018.77](https://doi.org/10.3144/expresspolymlett.2018.77)
- [9] Petrie E. M., *Handbook of adhesives and sealants*. The McGraw-Hill Companies, Inc., 1999
- [10] Marques E.A.S et al., *Introdução às ligações adesivas estruturais*, Quântica Editora – Conteúdos Especializados, Lda., 2021
- [11] Sun, S.; Li, M.; Liu, A., A review on mechanical properties of pressure sensitive adhesives, *International Journal of Adhesion and Adhesives*, **2013**, 41, 98-106. [dx.doi.org/10.1016/j.ijadhadh.2012.10.011](https://doi.org/10.1016/j.ijadhadh.2012.10.011) [15]
- [12] Engels, H.-W., et al., Polyurethanes: Versatile Materials and Sustainable Problem Solvers for Today's Challenges, *Angewandte Chemie International Edition*, **2013**, 52, 9422-9441. [dx.doi.org/10.1002/anie.201302766](https://doi.org/10.1002/anie.201302766)

- [13] Cao A. L. et al., Study of Properties of One-Component Moisture-Curable Polyurethane and Silane Modified Polyurethane Adhesives, *Journal of Adhesion Science and Technology*, **2012**, 26, 1395-1405. [dx.doi.org/10.1163/156856111X618272](https://doi.org/10.1163/156856111X618272)
- [14] Persson, A.-M.M.R.; Andreassen, E., Cyclic Compression Testing of Three Elastomer Types - A Thermoplastic Vulcanizate Elastomer, a Liquid Silicone Rubber and Two Ethylene-Propylene-Diene Rubbers, *Polymers*, **2022**, 14. [dx.doi.org/10.3390/polym14071316](https://doi.org/10.3390/polym14071316)
- [15] Czech, Z., Synthesis and cross-linking of acrylic PSA systems, *Journal of Adhesion Science and Technology*, **2007**, 21, 625-635. [dx.doi.org/10.1163/156856107781192337](https://doi.org/10.1163/156856107781192337)
- [16] Awaja, F. et al., Adhesion of polymers, *Progress in Polymer Science*, **2009**, 34, 948-968. [dx.doi.org/10.1016/j.progpolymsci.2009.04.007](https://doi.org/10.1016/j.progpolymsci.2009.04.007)
- [17] Polymer Database, Encyclopedia of Adhesive Technology, [Online]. Available: <https://polymerdatabase.com/Adhesives/Gluepedia%20A.html>., [Accessed: 30-Sep-2022]
- [18] Pethrick, R. A., Design and ageing of adhesives for structural adhesive bonding – A review, *Proceedings of the Institution of Mechanical Engineers, Part L: Journal of Materials: Design and Applications*, **2015**, 229, 349-379. [dx.doi.org/10.1177/1464420714522981](https://doi.org/10.1177/1464420714522981)
- [19] Pinto A. M. G., Ligações adesivas entre materiais poliméricos com e sem alteração superficial dos substratos, PhD Thesis, *Faculdade de Engenharia da Universidade do Porto*, Porto, Portugal, **2007**
- [20] Banea, M. D.; da Silva, L. F. M., Adhesively bonded joints in composite materials: An overview, *Proceedings of the Institution of Mechanical Engineers, Part L: Journal of Materials: Design and Applications*, **2009**, 223, 1-18. [dx.doi.org/10.1243/14644207JMDA219](https://doi.org/10.1243/14644207JMDA219)
- [21] Jin, X. et al., Challenges and Solutions for Joining Polymer Materials, *Macromolecular Rapid Communications*, **2014**, 35, 1551-1570. [dx.doi.org/10.1002/marc.201400200](https://doi.org/10.1002/marc.201400200)
- [22] Mittal K. L., Handbook of adhesive technology, 2nd ed, *Marcel Dekker, Inc.*, New York, U.S.A, 2003
- [23] Schaubroeck D., Surface modifications of epoxy resins to improve the adhesion towards electroless deposited copper, *PhD Thesis, Gent, Belgium*, **2015**
- [24] Maia B. S., Study on the effect of surface energy of polypropylene/polyamide12 polymer hybrid matrix reinforced with virgin and recycled carbon fiber, Master Thesis, *Faculty of Forestry, University of Toronto, Toronto, Canada*, **2017**

- [25] Davis M. J.; Bond D. A., The importance of failure mode identification in adhesive bonded aircraft structures and repairs, *Aircraft Structural Integrity Section*, Melbourne, Australia
- [26] Biolin Scientific, Cohesive vs. adhesive failure in adhesive bonding, **2021** [Online]. Available:<https://www.biolinscientific.com/blog/cohesive-vs.-adhesive-failure-in-adhesive-bonding>. [Accessed: 15-Jun-2022]
- [27] Baldan, A., Adhesively-Bonded Joints and Repairs in Metallic Alloys, Polymers and Composite Materials: Adhesives, Adhesion Theories and Surface Pretreatment, *Journal of Materials Science*, **2004**, 39, 1-49. [dx.doi.org/10.1023/B:JMSC.0000007726.58758.e4](https://doi.org/10.1023/B:JMSC.0000007726.58758.e4)
- [28] Kwok, D. Y.; Neumann, A. W., Contact angle measurement and contact angle interpretation, *Advances in Colloid and Interface Science*, **1999**, 81, 167-249. [dx.doi.org/10.1016/S0001-8686\(98\)00087-6](https://doi.org/10.1016/S0001-8686(98)00087-6)
- [29] Baldan, A., Adhesion phenomena in bonded joints, *International Journal of Adhesion and Adhesives*, **2012**, 38, 95-116. [dx.doi.org/10.1016/j.ijadhadh.2012.04.007](https://doi.org/10.1016/j.ijadhadh.2012.04.007)
- [30] Kwok, D. Y. et al., Contact Angle Measurements and Contact Angle Interpretation. 1. Contact Angle Measurements by Axisymmetric Drop Shape Analysis and a Goniometer Sessile Drop Technique, *Langmuir*, **1997**, 13, 2880-2894. [dx.doi.org/10.1021/la9608021](https://doi.org/10.1021/la9608021)
- [31] Molitor, P.; Barron, V.; Young, T., Surface treatment of titanium for adhesive bonding to polymer composites: a review, *International Journal of Adhesion and Adhesives*, **2001**, 21, 129-136. [dx.doi.org/10.1016/S0143-7496\(00\)00044-0](https://doi.org/10.1016/S0143-7496(00)00044-0)
- [32] Palmieri, F. L. et al., Laser ablation surface preparation for adhesive bonding of carbon fiber reinforced epoxy composites, *International Journal of Adhesion and Adhesives*, **2016**, 68, 95-101. [dx.doi.org/10.1016/j.ijadhadh.2016.02.007](https://doi.org/10.1016/j.ijadhadh.2016.02.007)
- [33] Hamdi, M.; Poulis, J. A., Effect of UV/ozone treatment on the wettability and adhesion of polymeric systems, *The Journal of Adhesion*, **2021**, 97, 651-671. [dx.doi.org/10.1080/00218464.2019.1693372](https://doi.org/10.1080/00218464.2019.1693372)
- [34] Modic, M. et al., Aging of plasma treated surfaces and their effects on platelet adhesion and activation, *Surface and Coatings Technology*, **2012**, 213, 98-104. [dx.doi.org/10.1016/j.surfcoat.2012.10.026](https://doi.org/10.1016/j.surfcoat.2012.10.026)
- [35] Encinas, N. et al., Control of Wettability of Polymers by Surface Roughness Modification, *Journal of Adhesion Science and Technology*, **2010**, 24, 1869-1883. [dx.doi.org/10.1163/016942410X51104233](https://doi.org/10.1163/016942410X51104233)

- [36] USA KINO, Contact angle, wetting, and spreading - Theory of surface tension, contact angle, wetting and work of adhesion (2), **2020**. [Online]. Available: http://www.uskino.com/articleshow_60.html. [Accessed: 21-May-2022]
- [37] Sun S.; Li M.; Liu. A., A review on mechanical properties of pressure sensitive adhesive, *International Journal of Adhesion & Adhesives*, **2013**, 41, 98-106. [dx.doi.org/10.1016/j.ijadhadh.2012.10.011](https://doi.org/10.1016/j.ijadhadh.2012.10.011)
- [38] Meadwell, J. et al., In Search of a Performing Seal: Rethinking the Design of Tight-Fitting Respiratory Protective Equipment Facepieces for Users with Facial Hair, *Safety and Health at Work*, **2019**, 10, 275-304. [dx.doi.org/10.1016/j.shaw.2019.05.001](https://doi.org/10.1016/j.shaw.2019.05.001)
- [39] Vieira T.; Lundberg J.; Erikson O., Evaluation of uncertainty on Shore hardness measurements of tyre treads and implications to, tyre/road noise measurements with the Close Proximity method, *Swedish National Road and Transport Research Institute (VTI)*, Linköping, Sweden
- [40] ISO, ISO 868 - Plastics and ebonite - Determination of indentation hardness by means of a durometer (Shore hardness), *International Organization for Standardization*, **2003**, 1-10.
- [41] Goglio L.; Rossetto M.; Dragoni E., Design of adhesive joints based on peak elastic stresses, *International Journal of Adhesion and Adhesives*, **2008**, 28, 427-435. [dx.doi.org/10.1016/j.ijadhadh.2008.04.001](https://doi.org/10.1016/j.ijadhadh.2008.04.001)
- [42] Loureiro A. L. et al., Comparison of the Mechanical Behavior Between Stiff and Flexible Adhesive Joints for the Automotive Industry, *The Journal of Adhesion*, **2010**, 86, 765-787. [dx.doi.org/10.1080/00218464.2010.482440](https://doi.org/10.1080/00218464.2010.482440)
- [43] ISO, ISO 4587 – Adhesives – Determination of lap-shear strength of rigid-to-rigid bonded assemblies, *International Organization for Standardization*, **2003**, 3, 1-10.
- [44] Lin Y.; Hui C. Y., Mechanics of contact and adhesion between viscoelastic spheres: An analysis of hysteresis during loading and unloading, *Journal of Polymer Science Part B: Polymer Physics*, **2002**, 40, 772-793. [dx.doi.org/10.1002/polb.10140](https://doi.org/10.1002/polb.10140)
- [45] Correia S. N., Mechanical behavior evaluation of adhesively bonded joints of aircraft structures, *Instituto Superior Técnico*, Lisboa, Portugal, **2016**